The Canadian Mineralogist
Vol. 34, pp. 301-324 (1996)

THE FORMATION OF QUARTZ SYENITE BY CRUSTAL CONTAMINATION AT MONT SHEFFORD AND OTHER MONTEREGIAN COMPLEXES, QUEBEC

JOHN D. LANDOLL AND KENNETH A. FOLAND

Department of Geological Sciences, Ohio State University, Columbus, Ohio 43210, U.S.A.

ABSTRACT

The Mont Shefford alkaline complex of southern Quebec contains mafic rocks and both silica-oversaturated and -undersaturated syenites. Chemical and isotopic studies examine the relationship of the various lithologies. Isotopic, major, and trace-element compositions are consistent with derivation of all lithologies from a common mafic parent, some of which evolved to a syenitic stage by fractional crystallization without significant contamination. Initial $^{87}Sr/^{86}Sr$ and $^{143}Nd/^{144}Nd$ values display distinct and systematic variations, with overall ranges of 0.70343 to 0.7099 and 0.51256 to 0.51269, respectively. These isotope ratios are negatively correlated and indicate evolution *via* combined assimilation and fractional crystallization (AFC), with the quartz syenite being the most strongly contaminated. The contamination probably occurred at a high level, perhaps near the level of intrusion. There is a clear relationship between the degree of silica saturation and the amount of contamination; this indicates that saturated and oversaturated rocks formed by AFC from a felsic undersaturated magma, whereas nepheline syenite formed in the absence of appreciable contamination. Such a process is shown to be consistent with the phase relations of Petrogeny's Residua System. Isotopic compositions for other Monteregian complexes containing oversaturated rocks are similar to those of Shefford and indicate derivation from similar time-integrated, mildly light-rare-earth-element-depleted mantle sources. At each location, there are negatively correlated variations in $^{87}Sr/^{86}Sr$ and $^{143}Nd/^{144}Nd$ that are consistent with production *via* AFC processes. Similar relationships have been documented at many other localities. Thus, production of oversaturated syenitic compositions from an undersaturated syenitic magma *via* AFC seems to be a common and important process in epizonal alkaline intrusive complexes.

Keywords: alkaline, oversaturated, undersaturated, quartz, nepheline, syenite, Petrogeny's Residua System, epizonal, contamination, igneous, Monteregian, assimilation, fractional crystallization, Mont Shefford, Quebec.

SOMMAIRE

Le complexe igné alcalin du mont Shefford (Québec) contient des roches mafiques et des termes évolués syénitiques, soit sursaturés, soit sous-saturés en silice. Notre étude des compositions chimiques et isotopiques visait à préciser les relations parmi les divers membres de cette association. Les données chimiques, portant sur les éléments majeurs et les éléments traces, et les rapports isotopiques, sont compatibles avec une dérivation de tous ces types de roches à partir d'un seul magma parent mafique; dans certains cas, la dérivation est due à une cristallisation fractionnée sans contamination importante. Les rapports initiaux $^{87}Sr/^{86}Sr$ et $^{143}Nd/^{144}Nd$ révèlent des variations distinctives et systématiques; ces rapports vont de 0.70343 à 0.7099 et de 0.51256 à 0.51269, respectivement. Ils font preuve d'une corrélation négative, et indiquent un mode d'évolution par une combinaison d'assimilation et de cristallisation fractionnée (ACF). Ce sont les échantillons de syénite quartzifère qui sont les plus fortement contaminés. Cette contamination a probablement eu lieu à faible profondeur, et peut-être même près du niveau de mise en place finale. Nous décelons un lien direct entre le degré de saturation en silice et le degré de contamination. Ainsi, les roches saturées et sursaturées se sont formées par ACF à partir d'un magma felsique sous-saturé, tandis que le magma syénitique à néphéline a cristallisé sans contamination importante. Un tel schéma d'évolution concorde avec les relations de phases bien connues du système quartz – néphéline – kalsilite. Les compositions isotopiques des autres complexes montérégiens qui contiennent des roches sursaturées en silice ressemblent à celles du mont Shefford, et indiquent une dérivation de sources mantelliques semblables, montrant dans chaque cas un faible appauvrissement en terres rares légères intégré sur une échelle temporelle. A chaque endroit, nous trouvons la même corrélation négative entre les rapports $^{87}Sr/^{86}Sr$ et $^{143}Nd/^{144}Nd$, qui semblent indiquer un mode de production par processus ACF. Des relations semblables ont été démontrées à plusieurs autres endroits. C'est donc dire que la production de compositions syénitiques quartzifères par processus ACF semble un phénomène généralisé et important dans les massifs intrusifs alcalins épizonaux.

(Traduit par la Rédaction)

Mots-clés: alcalin, sursaturé, sous-saturé, quartz, néphéline, syénite, système quartz – néphéline – kalsilite, épizonal, contamination, igné, Montérégien, assimilation, cristallisation fractionnée, mont Shefford, Québec.

Introduction

The Mont Shefford alkaline complex of the Monteregian Hills province in southern Quebec contains apparently cogenetic, silica-oversaturated and -undersaturated syenites. The formation of such associations from a common felsic magma is problematic because it is not consistent with closed-system fractionation. This is illustrated by phase-equilibrium relationships (*e.g.*, Tuttle & Bowen 1958, Fudali 1963, Hamilton & MacKenzie 1965) in Petrogeny's Residua System (quartz – nepheline – kalsilite), which preclude a magma from evolving by fractional crystallization across the feldspar join that separates oversaturated from undersaturated compositions. Recently however, Foland *et al.* (1993) demonstrated that it is possible for a felsic magma to evolve from undersaturation to oversaturation with equilibrium holding by coupled fractional crystallization and assimilation of granitic material. This model was proposed to apply to the formation of oversaturated–undersaturated felsic associations because the oversaturated representatives appear to have assimilated relatively larger amounts of granitic crust, as judged on the basis of isotopic tracers. The chemical and isotopic relationships among cogenetic oversaturated and undersaturated syenites, including those of the Mont Brome complex of the Monteregian Hills province (Foland *et al.* 1993, Chen *et al.* 1994), have been shown to be consistent with this hypothesis (Landoll *et al.* 1994, Landoll 1994). The present work on the Mont Shefford complex tests further the applicability of this basic hypothesis.

Geological Setting and Previous Work

The Mont Shefford complex (hereafter, simply "Shefford") is one of several of multi-intrusion alkaline complexes that constitute the Monteregian Hills province (Philpotts 1970, Eby 1987). The major intrusive complexes of this province extend in a roughly 200-km linear trend across southern Quebec and were intruded within a short episode in the Cretaceous (Foland *et al.* 1986). In general, the western Monteregian complexes are mafic and dominated by undersaturated rocks, whereas the eastern ones include more evolved compositions, including both oversaturated and undersaturated felsic rock-types.

Petrological relations

Shefford consists of a mafic mass that is cut by nepheline diorite and both silica-oversaturated and -undersaturated syenite (Fig. 1). The rock types have been described by Valiquette & Pouliot (1977), and the following descriptions serve to summarize that work while defining nomenclature with specific reference to analyzed samples. The nomenclature as defined by Valiquette & Pouliot (1977) is retained in this work in order to facilitate comparisons with previous work, for consistency with mapped units, and to facilitate discussion where distinctions between units would not be apparent under the IUGS system.

The "diorite" unit consists of diorite with subordinate amounts of gabbro, monzodiorite, quartz monzodiorite, and monzonite. The diorite and gabbro consist principally of plagioclase (some of which appears to be cumulate), kaersutite, and augite. Minor minerals include olivine, biotite, quartz, and feldspathoids. The monzonite is composed of plagioclase, alkali feldspar, biotite, and rare quartz with accessory titanite, apatite, and olivine. Samples #26, #134, and #59 consist primarily of euhedral to subhedral grains of unaltered plagioclase (up to 1 cm) that are poikilitically enclosed in amphibole. Biotite in sample #26 occurs as interstitial grains. Sample #58 is slightly more felsic than the others. Diorite samples #27 and #122 were collected from areas originally mapped as syenite (Fig. 1) and are similar to #58, but contain more biotite and pyroxene.

The nepheline diorite is medium-grained and consists principally of zoned plagioclase and amphiboles (magnesiohastingsite and kaersutite). Accessories include nepheline, sodalite, titanite, apatite, opaque phases, and cancrinite.

The pulaskite is medium- to coarse-grained nepheline syenite consisting of about 90% microperthitic to cryptoperthitic alkali feldspar and less than 5% nepheline. Mafic minerals include resorbed kaersutite coated with sodic magnesiohastingsite (Frisch 1970) and augite that is rimmed by a green sodic pyroxene. Accessories are apatite, titanite, opaque phases, and zircon. The pulaskite is associated with three other facies of nepheline syenite: micropulaskite, foyaite, and laurdalite (porphyritic syenite with >10% feldspathoids). Because pulaskite is the dominant type of undersaturated syenite, and all samples analyzed in this work are either pulaskite or micropulaskite, pulaskite will be used to refer to all varieties of nepheline syenite. Samples #18, #29, #130, and #133 are typical of the pulaskite; the main differences are in grain size and amount of titanite. Sample #120 is a fine-grained and slightly porphyritic micropulaskite; plagioclase forms thin, elongate crystals that are generally more euhedral than in other pulaskite samples, and the amphiboles are partially resorbed, with a thin green rim. Samples #71 and #72 (from near the contact with nordmarkite; Fig. 1) contain lesser amounts of mafic minerals, titanite, and plagioclase, and some of the alkali feldspar is visibly perthitic, similar to that in the nordmarkite. Sample #19 comes from a complicated and heterogeneous outcrop a few meters from an apparent contact with country rock. It contains large (several cm) feldspar crystals and minor amounts of much smaller feldspar and mafic minerals. Importantly, it also contains a few per cent quartz and is, therefore, actually a quartz syenite. It is

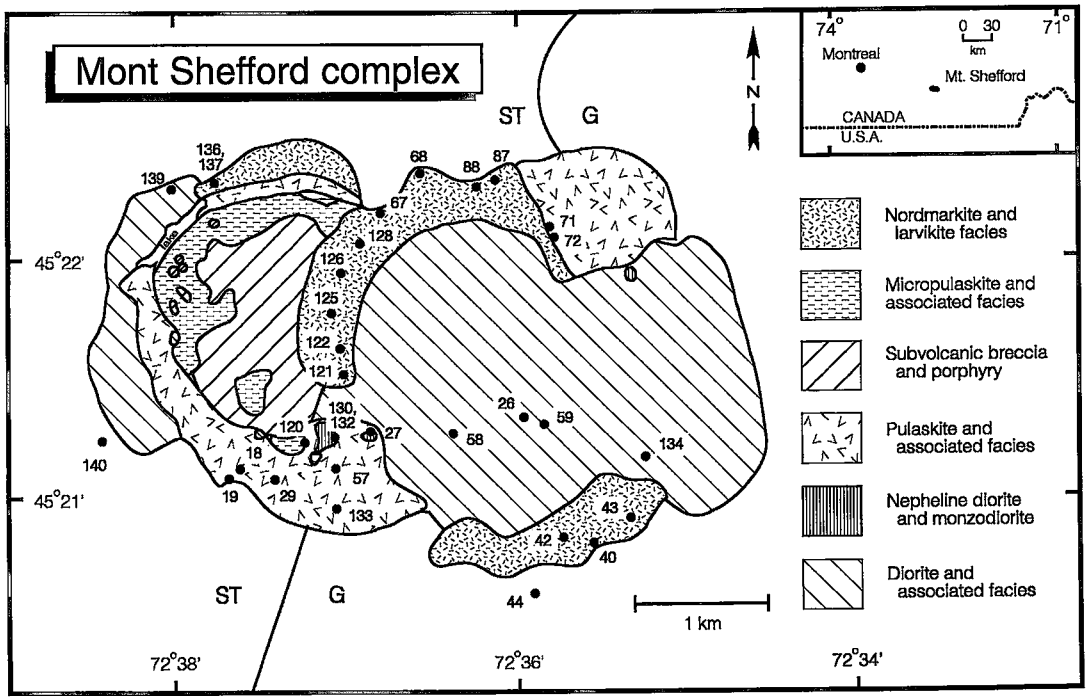

FIG. 1. Geological map of the Mont Shefford complex (after Valiquette & Pouliot 1977). Sample locations (denoted by the last digits of their notation from Table 1) are shown as solid circles. The heavy line outside the complex is the approximate contact between the Stanbridge Formation (ST) on the west and the Gilman Formation (Oak Hill Group, Gilman Formation, G) on the east [modified from Rickard (1991)].

grouped with the pulaskite because of its affinities (petrographic and chemical) with other pulaskite samples; the syenite within a few meters of #19 appears to be typical pulaskite. Sample #19 was analyzed to examine country rock – magma interactions near the contact.

A single mapped unit, nordmarkite (Fig. 1), consists of a quartz syenite facies ("nordmarkite" *sensu stricto*) and a syenitic to monzonitic ("larvikite") facies that is near silica saturation. Although these rock types are closely related and although previous investigators considered them together, new results show several important distinctions. The nordmarkite is composed of alkali feldspar with minor quartz (a few %), clinopyroxene, and Mn-rich olivine (less than 10%). Accessories include biotite, zircon, and opaque phases, but titanite, which is abundant in the nepheline syenite, is absent.

The larvikite facies is mineralogically similar to the nordmarkite, except that it contains little or no quartz; on the other hand, large feldspar crystals, some of which are plagioclase or contain partially resorbed plagioclase, seem to be of cumulate origin. In addition, some samples (*e.g.*, #136 and #137) contain a few crystals of titanite. Sample #139 contains more biotite and appears to be closer to a biotite monzonite petrographically, although the chemical composition is similar to those of other larvikite samples.

The subvolcanic breccia on the western side (Fig. 1) is composed of a variety of porphyries and diatreme breccias and likely represents a subvolcanic equivalent of the diorite (Valiquette & Pouliot 1977). The breccias were later reworked during a second brecciation event. No samples of this rock type were analyzed in the present study.

Geometrical and temporal relations

The geological map shown in Figure 1 presents only a generalized view of the actual distribution of the lithologies, because it is difficult to make field identification, and exposures are limited. Exposures made since mapping demonstrate somewhat more complex geometric relations and interfingering, particularly among felsic rock-types. In order to maintain a consistent nomenclature and emphasize the general chemical relationships (especially the state of silica saturation), the intrusive rocks are classified as diorite, nepheline diorite, pulaskite, nordmarkite, and larvikite.

The oversaturated rocks largely occur on the perimeter of the complex, whereas undersaturated ones typically occur in the interior. Exceptions are the pulaskite bodies in the northeastern and southern portions of the complex. An important feature of Shefford is that rocks mapped as nordmarkite occur both on the perimeter of the complex and in the interior. However, except in the northwestern part of the complex, the larvikite facies occupies interior portions (*e.g.*, samples #122, #126, #128), whereas nordmarkite occurs on the perimeter (*e.g.*, samples #67, #68, #40, #43). The positions of the nordmarkite and larvikite relative to country rocks suggest a link between access to wallrock and composition.

The order of intrusion of the units proposed by Valiquette & Pouliot (1977) is: diorite, nepheline diorite, pulaskite, subvolcanic breccia, micropulaskite, and nordmarkite (including the larvikite). These authors acknowledged difficulty in establishing this order, owing to the number and size of outcrops, the need to rely upon thin-section petrography for specific identification, and the lack of exposed contacts.

Country rocks

Shefford is emplaced into a thick sequence of Lower Cambrian and Middle Ordovician sedimentary and metasedimentary rocks (Rickard 1991, Slivitzky & St-Julien 1987). Contact metamorphism reached the hornblende hornfels facies (Valiquette & Pouliot 1977). Shefford is emplaced across a stratigraphic discontinuity (Fig. 1), represented in most places by a thrust fault (Slivitzky & St-Julien 1987) that separates phyllite, siltstone, and sandstone of the Oak Hill Group (mainly the Gilman Formation) along the eastern margin from the slate and carbonate of the Stanbridge Group along the western side. This fault could have served as the conduit for the magmas of Shefford, as was suggested for nearby Mont Brome (Doolan *et al.* 1982). Fault control of feeders has been proposed for other Monteregian intrusive complexes as well (Séguin 1982). Slivitzky & St-Julien (1987) indicated that the Oak Hill Formation under the eastern part of Shefford extends from 0 to 3 km, and the underlying Stanbridge, for another 2 km below the present level of erosion. Whereas the degree of homogeneity of the two stratigraphic units cannot be addressed in this study, new data coupled with those of Chen *et al.* (1994) and Wen (1994) show that the two formations have different compositions.

A highly complex zone consisting mostly of a fine-grained matrix and possible xenoliths of country rock is now exposed near the nordmarkite–diorite contact in the higher elevations of the northern part of the complex. The xenoliths range in size from a few cm to over 2 m in length. Some of these rocks appear similar in texture and xenolith content to the "rheomorphic breccia" described at Mont Brome by Philpotts (1970), suggesting that some of the country rock may have been mobilized during magma emplacement.

Age of Shefford

Eby (1984a) reported apatite fission-track dates of 119 ± 8 and 131 ± 8 Ma for a nepheline diorite and a diorite, respectively, and whole-rock Rb–Sr ages of 120.3 ± 1.0 Ma and 128.5 ± 3.0 Ma, respectively for the nordmarkite and pulaskite units. Foland *et al.* (1986) reported a $^{40}Ar/^{39}Ar$ plateau age of 123.5 ± 1.5 Ma for biotite from a diorite. Foland *et al.* (1986) concluded that this $^{40}Ar/^{39}Ar$ age was more precise than the previous fission-track dates and more reliable than the Rb–Sr whole-rock ages because they suffer from initial isotopic heterogeneities. Harper (1988) analyzed a nordmarkite sample and obtained a two-point (whole rock and alkali feldspar) Rb–Sr date of 124.7 Ma, and a concordant U–Pb zircon age of 126.0 Ma, with an estimated uncertainty of approximately 1 m.y. or less.

The age data for Shefford are consistent with the ages of other major Monteregian complexes which, with one exception, are within a very restricted range of 124 ± 1 Ma (Foland *et al.* 1986, 1989). Moreover, dates for the oldest (diorite) and youngest (nordmarkite) units are indistinguishable. This confirms a short interval of intrusion, as suggested for each Monteregian complex (Foland *et al.* 1986).

Chemical, isotopic, and petrogenetic studies

Previous chemical data (*e.g.*, Valiquette & Pouliot 1977, Eby 1985) agree well with those presented here; most differences are readily explained by heterogeneities. Eby (1985) reported a paucity of intermediate rocks (SiO_2 between 52 to 58%), attributed to the cumulate nature of the mafic rocks, and a bimodal distribution with respect to silica saturation in the syenites (*i.e.*, samples are either oversaturated or undersaturated) although the range is limited. Rare-earth-element (*REE*) patterns, with light-element enrichment (Eby 1985) are characteristic; the diorite and pulaskite have broadly similar patterns, whereas the nordmarkite has a pronounced negative Eu anomaly and a somewhat flatter heavy *REE* pattern. Based on various *REE* patterns, low concentrations of Sr and Ba in the nordmarkite, and contents of incompatible elements that are similar to those in the other syenites, Eby (1985) concluded that the nordmarkite formed from a magma that was different from the magmas parental to the other syenites.

Eby (1985) also concluded that the diorite formed from an alkali picritic melt similar to those that formed the gabbro and pyroxenite of the western Monteregian complexes (Eby 1984b), and that the highly undersaturated rocks formed from a second, basanitic mantle-derived magma intruded 10–15 m.y.

later. Based on $^{87}Sr/^{86}Sr$ ratios, Eby (1985) concluded that the Shefford magmas had interacted with crustal material and that the nordmarkite was derived by partial melting of the lower crust from heat supplied by ascending mafic magmas. Foland *et al.* (1986, 1988) used age, Sr, and Nd isotopic compositions of a Shefford diorite, and those of other Monteregian complexes, to conclude that the magma source was lithophile-element-depleted mantle, and that individual complexes formed in a short interval.

The nearby Mont Brome complex (hereafter "Brome") is similar to Shefford, and it is reasonable to suggest that they had similar origins. For Brome, Valiquette & Pouliot (1977) suggested that contamination of a saturated syenitic magma with gabbroic material caused it to become undersaturated and form the undersaturated syenites. In contrast, contamination with country rock caused the magma to become oversaturated, producing the quartz syenites. Chen *et al.* (1994) concluded that slightly undersaturated evolved magmas at Brome formed by fractional crystallization from a parental mantle-derived magma without significant crustal contamination. Some of the evolved magmas experienced combined assimilation and fractional crystallization (AFC) processes during emplacement in the upper crust that resulted in the

TABLE 1. MAJOR ELEMENT COMPOSITIONS OF SAMPLES FROM THE MONT SHEFFORD COMPLEX AND COUNTRY ROCK

No.	SiO_2	Al_2O_3	Fe_2O_3	MgO	CaO	Na_2O	K_2O	TiO_2	MnO	P_2O_5	TOTAL	Mg#
DIORITE												
26	47.33	21.15	8.23	4.45	11.57	3.46	0.56	2.30	0.17	1.19	100.41	54.2
134	48.87	21.84	6.80	3.83	11.63	3.45	0.60	1.97	0.16	1.16	100.31	55.1
58	46.93	16.01	10.28	6.58	8.87	4.56	1.50	2.96	0.23	2.26	100.18	58.3
59	45.34	20.11	7.61	6.34	12.46	3.45	0.66	2.69	0.19	1.47	100.32	64.5
27	51.76	19.86	6.94	3.90	8.30	5.06	1.08	2.07	0.17	0.81	99.95	55.1
122	52.20	18.86	7.46	4.17	7.03	5.10	2.13	1.88	0.18	0.80	99.81	54.9
NEPHELINE DIORITE												
132	49.01	15.87	11.00	4.80	7.84	5.34	2.37	2.34	0.36	1.30	100.23	48.5
PULASKITE												
120	59.67	19.91	3.68	0.72	3.00	7.36	4.16	0.94	0.27	0.22	99.93	28.7
133	61.59	18.63	3.58	0.91	2.55	6.86	4.36	0.82	0.39	0.30	99.99	33.4
29	61.98	18.86	3.62	0.81	2.25	7.00	4.18	0.87	0.36	0.26	100.01	30.9
130	58.74	19.05	4.81	1.10	3.36	6.97	3.95	1.18	0.29	0.44	99.89	32.3
18	61.26	19.39	3.29	0.64	2.25	7.56	4.33	0.66	0.19	0.22	99.79	28.9
19	66.36	17.84	1.95	0.48	1.10	5.45	6.09	0.41	0.16	0.09	99.93	33.4
57	61.61	18.98	3.35	0.85	2.33	7.10	4.36	0.76	0.19	0.25	99.78	34.7
71	63.16	19.42	2.56	0.36	1.36	6.62	5.53	0.56	0.17	0.09	99.83	22.6
72	63.48	19.48	2.46	0.63	1.30	6.17	5.30	0.74	0.16	0.12	99.84	34.7
LARVIKITE												
136	60.97	18.41	4.14	1.31	2.84	6.59	4.03	0.99	0.34	0.31	99.93	39.2
137	61.23	19.61	3.50	1.12	2.22	7.25	3.69	0.91	0.23	0.19	99.95	40.0
121	61.11	18.84	3.81	1.22	2.76	6.56	4.11	0.87	0.28	0.37	99.93	40.0
125	61.13	18.97	3.58	0.95	3.37	6.59	3.78	0.81	0.33	0.41	99.92	34.8
126	59.58	18.67	5.03	1.15	3.64	6.48	3.50	1.06	0.30	0.47	99.88	32.3
128	60.83	19.11	3.83	0.96	3.36	6.67	3.60	0.85	0.32	0.40	99.93	33.7
139	61.19	18.51	4.17	1.18	2.79	6.26	4.22	0.92	0.42	0.33	99.99	36.1
NORDMARKITE												
40	67.80	16.77	2.90	0.13	0.52	6.55	4.88	0.20	0.16	0.03	99.94	8.6
42	66.21	17.56	2.75	0.36	0.93	6.38	5.07	0.36	0.20	0.10	99.92	21.2
43	67.95	16.81	2.66	0.13	0.57	6.47	4.95	0.21	0.19	0.03	99.97	9.1
67	66.48	18.06	2.21	0.21	0.58	6.55	5.42	0.17	0.20	0.04	99.92	16.1
68	66.19	17.81	2.74	0.18	0.53	6.52	5.50	0.23	0.19	0.04	99.93	11.9
87	67.43	16.92	3.06	0.14	0.50	6.68	4.83	0.20	0.18	0.03	99.97	8.7
88	67.58	16.55	3.20	0.13	0.50	6.80	4.80	0.19	0.17	0.03	99.95	7.8
COUNTRY ROCK												
140	63.81	13.59	4.40	6.50	5.70	1.21	3.64	0.60	0.32	0.09	99.86	75.2
44	64.85	19.79	4.06	1.62	0.06	1.50	6.91	0.92	0.13	0.09	99.93	46.3

All values in weight %.

Mg# = (100 x Mg)/(Mg + Fe^{2+} + Mn) (molar), where the ratio Fe_2O_3/FeO = 0.15, by weight.

formation of the oversaturated rocks. Magmas not experiencing AFC continued to evolve by fractional crystallization and formed the undersaturated syenites. Thus, all rock units are related ultimately to a single parental magma-type, at least in terms of isotopic and general chemical compositions. The present study serves to explore this hypothesis further by demonstrating the importance of AFC and to put further constraints on the contamination processes.

Samples and Analytical Methods

A total of 32 samples representing all major units (except the subvolcanic breccia) were chosen for chemical and isotopic analysis from more than 100 specimens collected and examined. Sample #26 was studied previously by Foland *et al.* (1988), who reported Sr and Nd isotope data for this sample that are consistent with those from the present study, but of much lower precision. Sample locations are shown on Figure 1. The analyzed rocks do not display any extensive alteration by a subsolidus hydrothermal process.

Concentrations of major and trace elements were determined by X-ray-fluorescence spectroscopy at the University of Manchester. Because volatile weight-loss and ferrous iron determinations were not performed, analytical results are reported on a volatile-free basis, with total iron as Fe_2O_3. Rb–Sr and Sm–Nd isotopic analyses were performed at Ohio State University following the procedures discussed in Foland & Allen (1991). Rb analyses were performed on a Nuclide 12–SU–90 mass spectrometer, whereas those for Sr, Sm, and Nd were made on a Finnigan–MAT 261A with nine collectors. Analyses of the SRM–987 and "La Jolla" standards at the time the Shefford samples were analyzed yielded $^{87}Sr/^{86}Sr$ and $^{143}Nd/^{144}Nd$ ratios of 0.710243 (±0.000010, one sigma of the population; 147 analyses) and 0.511843 (±0.000005; 98 analyses). The one-sigma external precision of $^{143}Nd/^{144}Nd$ analyses is taken to be ±0.000004, on the basis of multiple runs of samples from the same rock unit or lava flow.

An age of 123.5 Ma (with an uncertainty of 1.5 m.y.) is used to calculate initial isotope ratios. With the exception of the nordmarkite samples with high

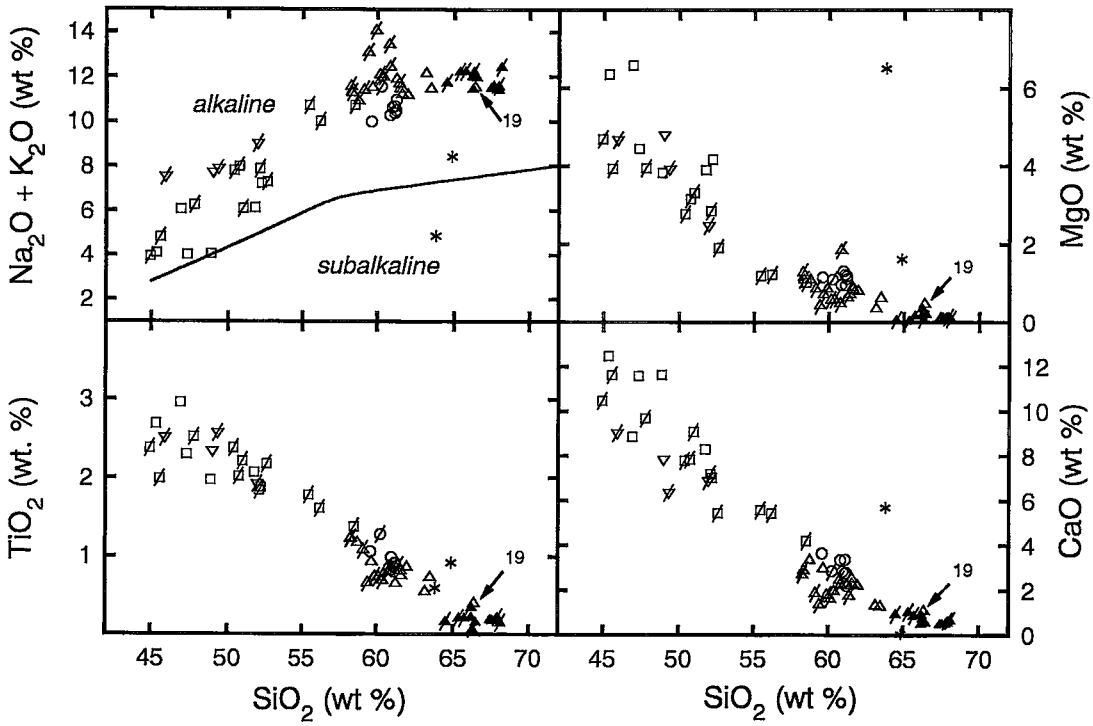

FIG. 2. Harker diagrams for Mont Shefford samples. Symbols and notation for this and all subsequent figures are: □: diorite, ▽: nepheline diorite, △: pulaskite, ○ larvikite, ▲: nordmarkite, *: country rock, and two-digit numbers (last two of notation in tables) to identify specific samples emphasized in the text. Literature values [from Valiquette & Pouliot (1977) and Eby (1985)] are shown with symbols having a slash (/). The alkaline–subalkaline boundary is from Miyashiro (1978). The samples display trends consistent with evolution from a mafic parent *via* fractional crystallization. Although all Shefford rocks are alkaline, none analyzed in this study are peralkaline.

Rb/Sr, uncertainty in age does not significantly affect the calculated initial ratios. However, any age significantly greater than 125 Ma produces unrealistically low initial $^{87}Sr/^{86}Sr$ for nordmarkite samples #87 and #88. Regressions for the isochron analyses are the model-I treatment of the McIntyre cubic least-squares method (Brooks *et al.* 1972).

Results

Major-element chemistry

Major-element concentrations for Shefford and the country rocks are given in Table 1, and some important relationships are illustrated in Figures 2 and 3. Mg-numbers [100 Mg/(Mg + Fe^{2+} + Mn)] range from 54 to 65 for diorite, 23 to 35 for pulaskite, 32 to 40 for larvikite, and 8 to 22 for nordmarkite (Table 1, Fig. 3). The highest Mg-number, 65, shows that the most primitive melt is rather Fe-rich, as observed for Monteregian complexes in general (*e.g.*, Greenwood & Edgar 1984, Eby 1985, Bédard *et al.* 1987, Chen *et al.* 1994). Pulaskite sample #19 (from the heterogeneous outcrop described above) has a relatively high Mg-number (33), unlike the nordmarkite suite. The larvikite samples have Mg-numbers similar to those of pulaskite, indicating that larvikite and pulaskite formed at similar stages of evolution, but that the nordmarkite is considerably more evolved. Nordmarkite #42 has a Mg-number considerably higher than other nordmarkite samples, which suggests that either it is less evolved or had a different evolution.

Chemical parameters display coherent trends from the mafic to the evolved rocks (Figs. 2–4). These relationships are similar (with only a few exceptions) to those reported previously for Brome and other Monteregian and similar complexes in other provinces. The diorite and pulaskite samples are slightly richer in Mg and Ca, respectively (Fig. 2), compared to those reported by Eby (1985). In addition, Eby (1985) noted that the Shefford nordmarkite is unique among quartz-bearing rocks in the Monteregian Hills in that it is peralkaline. In contrast, none of the samples analyzed in this study are peralkaline, although some have (Na + K)/Al (molar) values between 0.9 and 1.0. There is a marked deficiency of oversaturated rocks of

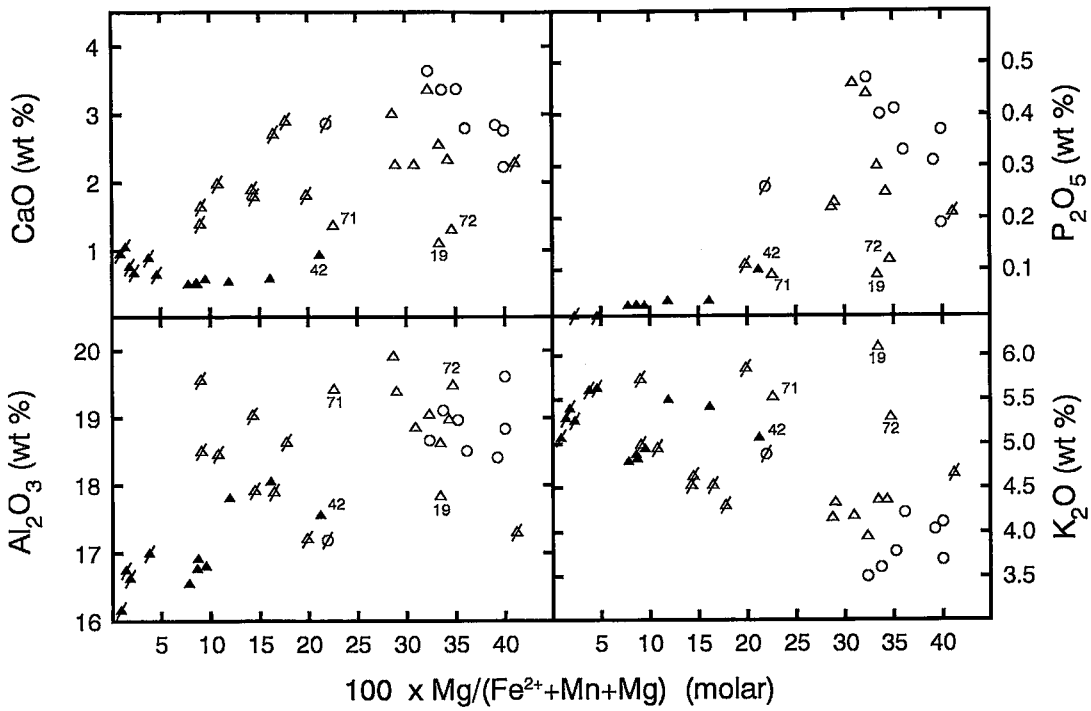

FIG. 3. Variations of CaO, Al_2O_3, P_2O_5, and K_2O *versus* Mg number for evolved samples. Symbols as in Fig. 2. Depletion trends are consistent with fractional crystallization. Scatter in the pulaskite and larvikite samples reflects crystal accumulation. The nordmarkite samples are considerably more evolved than the other syenites.

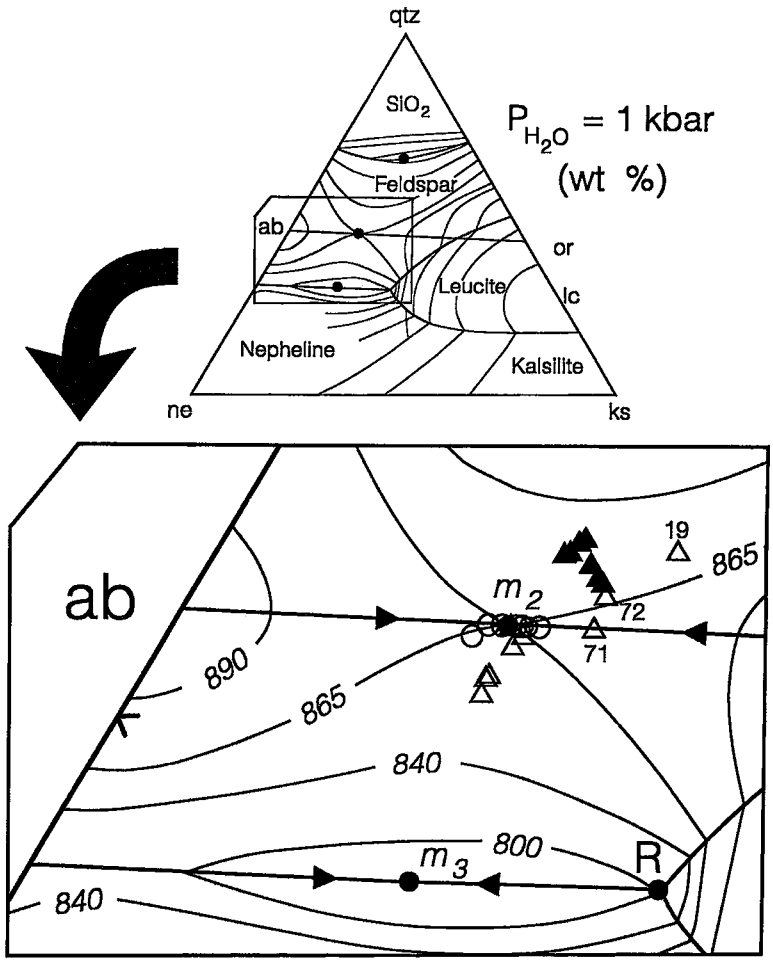

FIG. 4. Compositions (wt. %) of felsic rocks in terms of Petrogeny's Residua System (quartz – nepheline – kalsilite, qtz–ne–ks). Phase boundary curves, liquidus isotherms, and the minima in the granite and phonolite systems (solid dots) for 1 kbar $P(H_2O)$ are shown in the reference triangle at the top (after Henderson 1984). The enlargement (liquidus isotherms in °C) shows projected sample compositions, in which the ternary components are calculated from CIPW norms. Symbols as in Fig. 2. The minimum on the feldspar join (solid dot, m_2) is obscured by the larvikite samples; m_3 is the minimum in the phonolite system. Oversaturated and undersaturated samples plot along the thermal valley toward the minima in their respective systems. The state of silica saturation inferred from this diagram agrees well with that based on petrography. Pulaskite samples #19 and #72 plot in the granite system, and #71 plots on the feldspar join. Sample #19 contains modal quartz and is only nominally a pulaskite, as explained in the text. Samples #71 and 72 are from near the contact with nordmarkite.

intermediate composition Shefford (*e.g.*, Fig. 2). A similar paucity in oversaturated intermediate rocks apparent at Brome was attributed by Eby (1985) to crystal accumulation in the diorite. However, oversaturated intermediate compositions are not observed or are under-represented at Brome and similar complexes elsewhere, where undersaturated intermediate compositions are common and form part of a more complete evolutionary series. This suggests that the "compositional gap" is more fundamental and related to the petrogenesis of the oversaturated syenites rather than crystal accumulation.

Major-element variations with silica are consistent with fractional crystallization controlling magma

compositions (Fig. 2). The mafic rocks display some scatter that is likely due to crystal accumulation. Pulaskite #19 has 66% SiO_2 and plots with the nordmarkite samples; it is likely contaminated, as discussed below. The three types of syenite plot as distinct groups with respect to Mg-number (Fig. 3). The pulaskite and larvikite generally show more scatter than the nordmarkite, and their fields in some cases overlap (Fig. 3), which probably reflects the effects of crystal accumulation. A similar conclusion was reached by Eby (1985), who noted that "least-squares and mixing calculations and trace-elements suggest that mineral accumulation played a role" in the formation of some of the syenites. Nordmarkite samples #67, #68, and #42 also have slightly higher K than other samples of nordmarkite. With the exception of pulaskite #19, these samples also have higher Al, consistent with feldspar accumulation.

Normative compositions

Normative compositions (Table 2) help quantify the degree of silica saturation, particularly for the felsic rocks. In the absence of actual measurements, a Fe_2O_3/FeO ratio (by weight) of 0.15 is assumed for norm calculations. Of course, the calculated norms are dependent upon this ratio, and the assumed value is basically arbitrary, although frequently used. This value is similar to those for the nordmarkite reported by Eby (1985), except one sample at 0.85. Four of the

TABLE 2. CIPW NORMATIVE COMPOSITIONS OF SAMPLES FROM THE MONT SHEFFORD COMPLEX AND COUNTRY ROCK

No.	Q	CO	OR	AB	AN	NE	DI	HY	OL	MT	IL	AP	TOTAL
DIORITE													
26			3.31	28.3	40.5	0.54	7.44		11.1	1.42	4.37	2.76	99.74
134			3.55	29.2	42.3		6.35	5.23	5.46	1.17	3.74	2.69	99.69
58			8.86	30.1	18.8	4.61	8.50		15.8	1.77	5.62	5.24	99.30
59			3.90	19.7	37.4	5.15	11.9		11.8	1.31	5.11	3.41	99.68
27			6.38	41.0	28.3	0.98	6.20		9.48	1.20	3.93	1.88	99.35
122			12.6	37.9	22.3	2.85	6.03		10.8	1.29	3.57	1.85	99.19
NEPHELINE DIORITE													
132			14.0	26.5	12.3	10.1	14.9		12.0	1.90	4.44	3.01	99.15
PULASKITE													
120			24.6	49.6	9.00	6.88	3.77		2.87	0.64	1.79	0.51	99.66
133			25.8	56.1	7.16	1.04	2.98		3.73	0.62	1.56	0.70	99.69
29			24.7	58.8	7.70	0.21	1.50		4.05	0.62	1.65	0.60	99.83
130			23.3	49.5	9.03	5.14	4.03		4.35	0.83	2.24	1.02	99.44
18			25.6	54.3	6.18	5.24	3.01		2.85	0.57	1.25	0.51	99.51
19	7.50	0.50	36.0	46.1	4.87			3.46		0.34	0.78	0.21	99.76
57			25.8	56.1	7.04	2.14	2.43		3.40	0.58	1.44	0.58	99.51
71		0.29	32.7	55.8	6.16	0.11			2.84	0.44	1.06	0.21	99.61
72	2.82	1.52	31.3	52.2	5.67			3.98		0.42	1.41	0.28	99.60
LARVIKITE													
136			23.8	55.8	8.75		2.77	1.37	3.75	0.71	1.88	0.72	99.55
137			21.8	59.3	9.77	1.13			4.79	0.60	1.73	0.44	99.56
121			24.3	55.5	9.82		1.22	2.46	3.14	0.66	1.65	0.86	99.61
125			22.3	55.8	11.0		2.55	3.72	1.11	0.62	1.54	0.95	99.59
126			20.7	54.8	11.5		2.94	1.01	4.49	0.87	2.01	1.09	99.41
128			21.3	56.4	11.6		2.10	2.92	2.10	0.66	1.61	0.93	99.62
139			24.9	53.0	9.94		1.47	6.95	0.13	0.72	1.75	0.77	99.63
NORDMARKITE													
40	8.12		28.8	55.4	1.95		0.39	4.03		0.50	0.38	0.07	99.64
42	5.85	0.13	30.0	54.0	3.96			4.41		0.47	0.68	0.23	99.73
43	8.49		29.3	54.8	2.21		0.37	3.75		0.46	0.40	0.07	99.85
67	4.79	0.46	32.0	55.4	2.62			3.61		0.38	0.32	0.09	99.67
68	4.24	0.26	32.5	55.2	2.37			4.14		0.47	0.44	0.09	99.71
87	7.08		28.5	56.5	1.92		0.32	4.34		0.53	0.38	0.07	99.64
88	6.89		28.4	57.5	0.46		1.61	3.82		0.55	0.36	0.07	99.66
COUNTRY ROCK													
140	20.1		21.5	10.2	20.9		5.45	19.2		0.76	1.14	0.21	99.46
44	25.3	9.84	40.8	12.7				8.27		0.70	1.75	0.11	99.47

Calculations assume Fe_2O_3/FeO= 0.15, by weight.

pulaskite samples reported by Eby (1985) have Fe_2O_3/FeO ratios from 0.19 to 0.25, and three others range from 0.48 to 0.57. The former values are only slightly higher than 0.15 and have a minimal effect on the degree of saturation, and those from the latter group are similar to the mafic rocks from Eby (1985). For the felsic rocks, the FeO/Fe_2O_3 value is not especially important in view of their low iron contents. More importantly, calculated normative compositions in Table 2 (in terms of silica saturation) agree very well with rock type and modal petrography.

Overall, there is a moderate range in degree of saturation from about 7% *ne* to about 8% *qtz*. The diorite is nearly saturated to moderately undersaturated (0.5% to 5% *ne*; sample #134 contains 5% *hy*). With two exceptions, the pulaskite is near saturation, ranging from 3% *qtz* to about 4% *ne*. The larvikite is just at saturation, being neither *qtz* nor *ne*-normative (except for #137, with 1.1% *ne*). The nordmarkite is oversaturated, ranging from 4% to 8% *qtz*.

In Petrogeny's Residua System (Fig. 4), felsic samples bridge the feldspar join near its minimum and extend into both the granite and phonolite systems along the thermal valleys. The larvikite samples cluster around the minimum on the join, particularly if uncertainties in the position of the minimum and the

TABLE 3. TRACE ELEMENT CONCENTRATIONS OF SAMPLES FROM THE MONT SHEFFORD COMPLEX AND COUNTRY ROCK

No.	Nb	Zr	Y	Sr	Rb	Zn	Cu	Ni	Cr	Ce	Nd	Sm	V	La	Ba	Sc
DIORITE																
26	70	487	26	1973	12.01	59	6	bd	5	118	51.73	9.504	221	43	343	bd
134	59	464	25	2041	7.820	50	20	bd	6	97	53.21	9.695	205	44	370	bd
58	141	205	79	1245	24.12	122	23	bd	11	361	143.2	24.08	332	133	2383	49
59	54	52	44	1936	8.890	52	24	bd	16	114	49.32	9.492	329	35	346	51
27	125	790	42	2735	24.34	86	8	bd	6	195	77.49	13.43	149	60	1086	19
122	134	629	38	1504	46.47	78	26	5	18	159	66.41	11.30	170	80	1308	17
NEPHELINE DIORITE																
132	181	624	40	1211	94.52	119	20	13	24	215	80.84	13.72	297	126	1172	32
PULASKITE																
120	308	1120	51	884.7	122.1	113	8	6	bd	278	77.33	11.67	66	135	1997	bd
133	291	704	64	824.2	88.86	118	6	bd	bd	261	111.3	17.24	70	150	3021	bd
29	299	822	66	829.3	86.16	125	bd	8	6	343	112.4	17.63	61	137	3220	bd
130	268	676	46	961.9	102.9	91	16	17	12	185	84.02	13.16	104	170	2865	28
18	364	876	43	871.3	134.6	110	12	bd	bd	308	104.8	15.76	75	140	1884	21
19	102	185	36	59.57	86.17	47	10	bd	bd	230	82.83	12.38	45	118	1018	11
57	255	431	54	879.5	84.15	91	10	bd	bd	207	86.84	13.70	82	114	2765	11
71	294	1018	30	196.7	144.1	53	bd	bd	bd	234	80.01	11.60	71	106	1200	bd
72	264	694	38	328.0	120.3	53	9	bd	5	248	106.3	15.39	88	204	1602	8
LARVIKITE																
136	209	551	41	805.0	122.1	124	bd	bd	bd	216	64.25	9.923	78	101	2732	bd
137	178	1294	32	766.3	92.73	121	13	13	bd	280	42.90	5.978	72	59	2922	bd
121	112	886	32	630.1	57.51	82	5	bd	bd	112	58.42	7.861	14	74	2187	bd
125	151	641	32	855.9	75.91	68	bd	bd	bd	208	52.23	7.696	37	107	1647	bd
126	151	698	32	826.4	75.49	90	15	bd	8	194	47.38	6.932	75	116	1343	bd
128	197	715	39	693.3	73.76	90	5	bd	bd	201	50.21	7.739	59	79	1432	24
139	119	597	37	1057	67.87	103	8	8	bd	160	56.87	9.369	48	65	1975	bd
NORDMARKITE																
40	212	366	22	1.863	114.6	53	bd	bd	bd	206	87.83	10.81	13	155	29	17
42	194	831	44	134.2	110.3	84	bd	bd	bd	308	72.52	9.999	32	118	694	21
43	277	705	30	2.101	161.2	56	bd	bd	bd	269	114.6	14.47	10	129	12	11
67	96	395	15	3.508	87.04	30	bd	bd	bd	265	93.18	9.720	10	194	bd	23
68	192	975	32	3.203	94.03	44	bd	bd	bd	313	143.0	15.98	17	236	bd	bd
87	274	509	20	1.814	118.8	50	bd	bd	bd	413	100.5	13.46	bd	162	bd	bd
88	330	744	31	1.616	150.8	75	bd	bd	5	349	105.2	14.11	10	189	bd	20
COUNTRY ROCK																
140	21	188	22	156.8	115.8	143	44	44	117	81	15.95	2.896	184	36	1196	17
44	21	490	40	73.10	173.7	46	15	26	78	139	13.11	3.056	137	17	1312	17

All concentrations given in ppm. Values below detection reported as "bd." Detection limits are: 5 ppm for Zn, Cu, Ni, Cr, Sc, and 10 ppm for Nb, Zr, Y, Ce, V, La, Ba.

Rb, Sr, Sm, Nd analyses by isotope dilution at Ohio State University; all others by XRF at the University of Manchester.

norm calculation are considered. The oversaturated samples trend along the valley toward the granite minimum. Pulaskite #19 plots with nearly the highest values of *qtz* and *ks*, and pulaskite #72 also contains relatively high proportions of *qtz* and *ks*. The undersaturated samples show much less variation, and extend from near the feldspar minimum toward the phonolite minimum along the thermal valley.

Trace-element concentrations

Trace-element concentrations (Table 3, Fig. 5) are similar to those reported by Eby (1985). The concentrations of compatible elements generally decrease with increasing silica, consistent with fractional crystallization. For example, the diorite contains about 150 to 330 ppm V (Fig. 5), whereas the felsic rocks have considerably lower concentrations (from 14 to 78 ppm, 45 to 104 ppm, and 8 to 32 ppm in the larvikite, pulaskite, and nordmarkite, respectively). The diorite has variable Sr contents (Fig. 5), from about 1500 to 2730 ppm. Sr concentrations of six of the pulaskite samples are fairly uniform (825 to 960 ppm), but two samples (#71 and 72) are lower (200 and 330 ppm), whereas anomalous pulaskite #19 is much lower at 60 ppm. For Ba (Fig. 5), the pulaskite ranges from 1020 to 3230 ppm, and the larvikite, from 1340 to 2920 ppm. The nordmarkite is much lower (30 ppm or less), except for #42, at 700 ppm. Thus, sample #42 is distinguished from the remaining nordmarkite samples by trace elements. Significantly higher Sr contents of the larvikite distinguishes it from the nordmarkite. The low concentrations of Sr and Ba in the nordmarkite is taken to be a result of extensive crystal-fractionation.

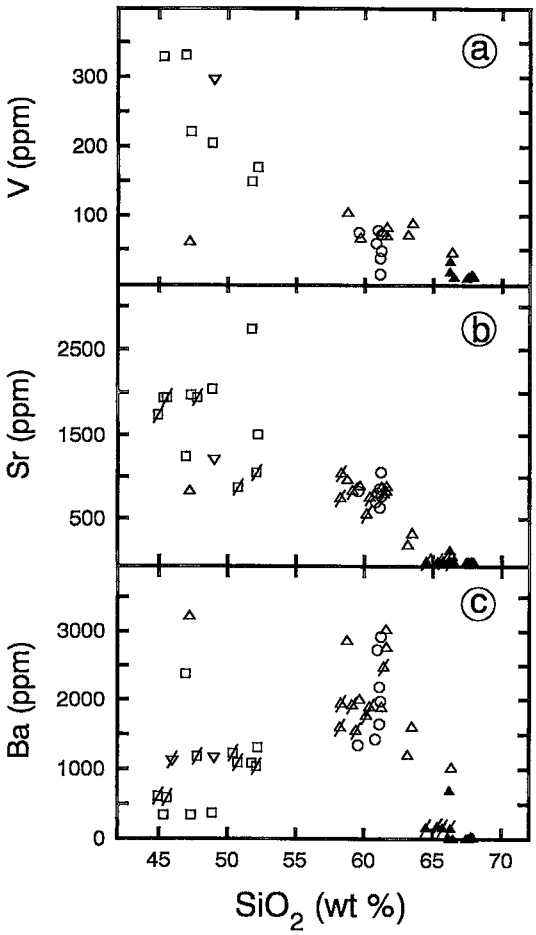

FIG. 5. Variations of V, Sr, and Ba with SiO_2 for Shefford samples. Symbols as described in Fig. 2.

Isotopic results

Results of the isotopic analyses are given in Table 4. Three Rb–Sr analyses are shown for nordmarkite sample #43. This sample gave a high calculated initial $^{87}Sr/^{86}Sr$ and was re-analyzed as a check. The repeat analyses did not replicate well (Table 4) for unknown reasons, including the possibility of a grossly heterogeneous sample. Thus, the Sr-isotopic results for #43 are not considered sufficiently reliable and are not used.

Calculated initial ratios for both $^{87}Sr/^{86}Sr$ and $^{143}Nd/^{144}Nd$ show significant intra- and interunit variations that are inversely correlated (Fig. 6) and these are the focus of the following discussion. Typical uncertainties for calculated initial isotope ratios are: 0.000004 for $^{143}Nd/^{144}Nd$ for all samples, 0.000002 for $^{87}Sr/^{86}Sr$ for all samples except the nordmarkite, and 0.004 for $^{87}Sr/^{86}Sr$ for nordmarkite samples. Values of $^{87}Sr/^{86}Sr$ range from 0.70343 to 0.7099, whereas the ratio $^{143}Nd/^{144}Nd$ ranges from 0.512558 to 0.512688 (ε_{Nd} = +1.6 to +4.1). Nepheline diorite #132 has the lowest value of $^{87}Sr/^{86}Sr$ (0.70343) and highest value of $^{143}Nd/^{144}Nd$ (0.512682). The diorite samples have a somewhat higher $^{87}Sr/^{86}Sr$ value (0.70369 to 0.70418) and a lower $^{143}Nd/^{144}Nd$ value (0.512656 to 0.512672). With the exception of #19, pulaskite samples give a low $^{87}Sr/^{86}Sr$ value (0.70353 to 0.70396) and a fairly high $^{143}Nd/^{144}Nd$ value (0.512688 to 0.512646); #19 has a distinctly higher $^{87}Sr/^{86}Sr$ value, 0.7086, and a slightly lower $^{143}Nd/^{144}Nd$ value, 0.512641. These values are similar to those for the nordmarkite and suggest that sample #19 underwent a similar evolution to the nordmarkite (*i.e.*, contamination). Larvikite samples overlap the pulaskite, but range to higher values of $^{87}Sr/^{86}Sr$ (0.70370 to 0.70407) and lower values of $^{143}Nd/^{144}Nd$ (0.512664 to 0.512632). Larvikite #139 is distinct at 0.70443 and 0.512258, respectively. The nordmarkite samples give $^{87}Sr/^{86}Sr$ values (albeit with significant analytical uncertainties) that are quite

TABLE 4. Nd AND Sr ISOTOPIC DATA FOR SAMPLES FROM THE MONT SHEFFORD COMPLEX AND COUNTRY ROCK

No.	$^{87}Rb/^{86}Sr$	Sr	$^{87}Sr/^{86}Sr$[a]	$(^{87}Sr/^{86}Sr)_i$[b]	$^{147}Sm/^{144}Nd$	Nd	$^{143}Nd/^{144}Nd$[a]	$(^{143}Nd/^{144}Nd)_i$[b]	ε_{Nd}[c]
DIORITE									
26	0.01759	1973	0.703740 (10)	0.703709 (10)	0.1111	51.73	0.512746 (6)	0.512656	3.45
134	0.01107	2041	0.703711 (8)	0.703692 (8)	0.1102	53.21	0.512745 (7)	0.512656	3.45
58	0.05604	1245	0.704274 (12)	0.704176 (12)	0.1016	143.2	0.512749 (5)	0.512667	3.66
59	0.01329	1936	0.703734 (13)	0.703711 (13)	0.1164	49.32	0.512750 (7)	0.512656	3.45
27	0.02574	2735	0.703881 (9)	0.703836 (9)	0.1048	77.49	0.512747 (9)	0.512662	3.57
122	0.08939	1504	0.703883 (9)	0.703726 (9)	0.1029	66.41	0.512755 (7)	0.512672	3.76
NEPHELINE DIORITE									
132	0.2258	1211	0.703828 (10)	0.703432 (11)	0.1026	80.84	0.512765 (5)	0.512682	3.96
PULASKITE									
120	0.3990	884.7	0.704391 (5)	0.703691 (10)	0.09120	77.33	0.512746 (5)	0.512672	3.76
133	0.3118	824.2	0.704277 (6)	0.703730 (9)	0.09365	111.3	0.512744 (6)	0.512668	3.69
29	0.3005	829.3	0.704266 (8)	0.703739 (11)	0.09486	112.4	0.512749 (5)	0.512672	3.76
130	0.3093	961.9	0.704070 (8)	0.703527 (11)	0.09465	84.02	0.512764 (7)	0.512688	4.08
18	0.4469	871.3	0.704505 (9)	0.703721 (14)	0.09092	104.8	0.512755 (7)	0.512682	3.96
19	4.188	59.57	0.715931 (10)	0.708580 (97)	0.09253	82.83	0.512716 (6)	0.512641	3.16
57	0.2767	879.5	0.704260 (14)	0.703759 (15)	0.09539	86.84	0.512723 (9)	0.512646	3.26
71	2.120	196.7	0.707685 (17)	0.703964 (52)	0.08765	80.01	0.512739 (6)	0.512668	3.69
72	1.061	328.0	0.705552 (10)	0.703690 (26)	0.07583	106.3	0.512732 (5)	0.512671	3.74
LARVIKITE									
136	0.4389	805.0	0.704550 (11)	0.703780 (15)	0.09337	64.25	0.512724 (7)	0.512649	3.31
137	0.3500	766.3	0.704687 (7)	0.704073 (11)	0.08425	42.90	0.512702 (8)	0.512634	3.02
121	0.2640	630.1	0.704260 (8)	0.703797 (10)	0.08136	58.42	0.512730 (6)	0.512664	3.61
125	0.2565	855.9	0.704162 (10)	0.703712 (12)	0.08909	52.23	0.512704 (5)	0.512632	2.98
126	0.2642	826.4	0.704165 (8)	0.703701 (10)	0.08844	47.38	0.512727 (7)	0.512656	3.45
128	0.3077	693.3	0.704274 (10)	0.703734 (12)	0.09318	50.21	0.512726 (7)	0.512651	3.34
139	0.1857	1057	0.704752 (9)	0.704426 (10)	0.09608	56.87	0.512636 (7)	0.512558	1.55
NORDMARKITE									
40	183.6	1.863	1.03214 (4)	0.7099 (42)	0.07437	87.83	0.512676 (5)	0.512616	2.67
42	2.377	134.2	0.708358 (8)	0.704426 (55)	0.08336	72.52	0.512695 (5)	0.512628	2.91
43[d]	161.2	2.101	1.00646 (24)	0.7235 (37)	0.07632	114.6	0.512691 (6)	0.512629	2.92
	163.2	2.092	0.9907 (5)	0.7043 (38)					
	157.9	2.157	0.995 (1)	0.7186 (38)					
67	72.69	3.508	0.83627 (2)	0.7087 (17)	0.06307	93.18	0.512687 (5)	0.512636	3.06
68	86.20	3.203	0.86046 (2)	0.7092 (20)	0.06756	143.0	0.512678 (5)	0.512623	2.81
87	195.9	1.814	1.04830 (2)	0.7044 (45)	0.0810	100.5	0.512690 (5)	0.512625	2.85
88	283.1	1.616	1.20457 (13)	0.7077 (65)	0.08109	105.2	0.512692 (6)	0.512626	2.87
COUNTRY ROCK									
140	2.141	156.8	0.732854 (10)	0.72910 (5)	0.1097	15.95	0.511408 (7)	0.511319	-22.64
44	6.921	73.10	0.77823 (4)	0.76608 (16)	0.1410	13.11	0.512100 (10)	0.511986	-9.62

[a] Measured values normalized with $^{86}Sr/^{88}Sr = 0.119400$ or $^{146}Nd/^{144}Nd = 0.721900$. Uncertainties in the last digit(s) given in parentheses are two-standard deviations of the mean for in-run statistics.

[b] Calculated initial ratios using: an age of 123.5 ± 1.5 Ma; decay constants of 1.42×10^{-11} and 6.54×10^{-12} $year^{-1}$ for ^{87}Rb and ^{147}Sm, respectively; and an uncertainty of 0.5% in $^{87}Rb/^{86}Sr$. Uncertainties for initial $^{87}Sr/^{86}Sr$ ratios are one-sigma, calculated as described in Foland & Allen (1991); initial $^{143}Nd/^{144}Nd$ ratios have an assigned one-sigma uncertainty of 0.000004.

[c] Conventional epsilon notation for 123.5 Ma using present-day bulk earth values of 0.512638 and 0.1966 for the $^{143}Nd/^{144}Nd$ and $^{147}Sm/^{144}Nd$, respectively.

[d] Replicate Rb-Sr analyses listed for sample #43 do not agree well as explained in text. Nd analysis is considered reliable.

variable, and generally higher (0.7044 to 0.7099); their $^{143}Nd/^{144}Nd$ ratios are generally among the lowest (0.512616 to 0.512636). There is a clear broad correlation of calculated initial isotopic ratios, especially $^{143}Nd/^{144}Nd$, with rock type.

The compositions of both types of country rock are quite distinct from those of the Shefford rocks and each other (Tables 1, 4). The sample from the Stanbridge Formation (#140) has $^{87}Sr/^{86}Sr$ and $^{143}Nd/^{144}Nd$ values (calculated to 123.5 Ma) of 0.7291 and 0.51132,

respectively, and the one from the Gilman Formation (#44) has values of 0.7661 and 0.51199. It is clear that the two types of country rock near Shefford are different; similar differences also are observed a few km to the south near Brome (Chen *et al.* 1994, Wen 1994). Each formation is relatively homogeneous in $^{143}Nd/^{144}Nd$ (although minor variations are seen for the Stanbridge), but there are substantial variations in $^{87}Sr/^{86}Sr$. Ranges in $^{87}Sr/^{86}Sr$ and $^{143}Nd/^{144}Nd$ (at 123.5 Ma) for a total of eight samples are: 0.7313 to 0.7661 and 0.51195 to 0.51199, respectively, for the Gilman, and 0.7209 to 0.7507 and 0.51132 to 0.51164, respectively, for the Stanbridge.

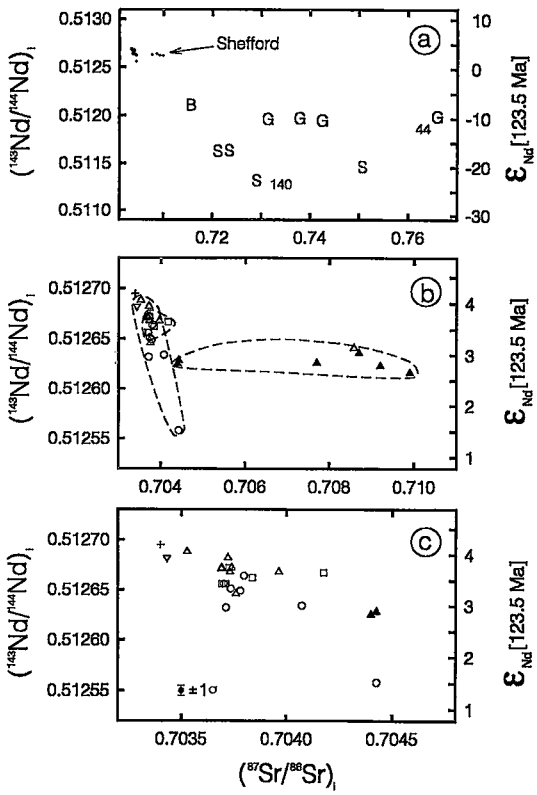

FIG. 6. Calculated initial $^{87}Sr/^{86}Sr$ and $^{143}Nd/^{144}Nd$ values for Shefford and country-rock samples. (a) Country-rock samples (S: Stanbridge Formation, G: Gilman Formation, B: Grenville basement). Samples #140 and #44 are from this study; other data are from Gilbert (1985), Chen *et al.* (1994), and Wen (1994). (b) Plot of all Shefford samples. The one-sigma error bar for the $^{143}Nd/^{144}Nd$ values is shown in (c). Uncertainties for initial $^{87}Sr/^{86}Sr$ values of the nordmarkite samples (except #42) are substantial (Table 4); all other rock types have uncertainties smaller than the symbol. Dashed lines outline the trends (mafic, undersaturated to saturated, and oversaturated) discussed in the text. (c) Enlargement of diagram showing variations for samples with low $^{87}Sr/^{86}Sr$. Note that isotope ratios are generally negatively correlated. Symbols: □: diorite, ∇: nepheline diorite, Δ: pulaskite, ○: larvikite, ▲: nordmarkite, and +: initial magma.

Significance of the Rb–Sr Results to the Age of Intrusion

Although the diorite, larvikite, and some pulaskite samples have Rb/Sr values too low to produce precise information about age, it is instructive to examine these data on an isochron diagram (Fig. 7a). The scatter is severe, showing clearly the very large variations in the present-day $^{87}Sr/^{86}Sr$ ratios that must reflect variations in the initial ratio.

For the pulaskite (Fig. 7b), there is considerable dispersion in the $^{87}Rb/^{86}Sr$ values, but the samples show excessive scatter and do not define a valid isochron. Even with the grossly deviant sample #19 omitted, the regression gives a date of 131.8 ± 1.8 Ma (Mean Standard Weighted Deviates, MSWD = 8.6), which cannot be considered reliable. Regression analyses involving various combinations where one or two samples are omitted result in an extremely wide range of dates, from about 130 to 181 Ma. The inevitable conclusion is that the pulaskite cannot be used to define an accurate Rb–Sr whole-rock age. The nordmarkite samples have much greater Rb/Sr values that also vary significantly. Although these data define a linear array, there are significant deviations (MSWD = 9.1) so that these samples do not define an acceptable isochron. The linear trend (or "errorchron") yields a date of 125.8 ± 0.3 Ma, which is consistent with an age of 123.5 ± 1.5 Ma. However, it cannot be considered fully reliable because of apparent heterogeneities in initial $^{87}Sr/^{86}Sr$; the true uncertainty is much greater than indicated by regression analysis. The Rb–Sr whole-rock analysis provides a more reasonable age, even with the initial heterogeneities, because these are small compared to *in situ* ^{87}Sr production.

Eby (1984a) reported a whole-rock isochron analysis of pulaskite samples that yielded a date of 128.5 ± 3.0 Ma and an initial $^{87}Sr/^{86}Sr$ ratio of 0.70365. However, there are obvious deviations from linearity even though the reported MSWD is only 0.36, which suggests a valid isochron; our regression using one-sigma errors gives a MSWD of 2.1. Eby (1984a) also reported an isochron analysis of four nordmarkite samples that yielded a date of 120.3 ± 1.0 Ma with an MSWD of 0.63 and an initial $^{87}Sr/^{86}Sr$ value of 0.70445. Unfortunately, the small number of samples limits this analysis, and variations will be masked by the high Rb/Sr ratios and analytical uncertainties on these. Both of these previous dates are compromised by isotopic heterogeneities, as verified with $^{143}Nd/^{144}Nd$ (Fig. 6) and the new data shown in Figure 7.

In sum, Shefford samples do not define reliable Rb–Sr whole-rock isochrons because of initial $^{87}Sr/^{86}Sr$ heterogeneities that also correlate well with

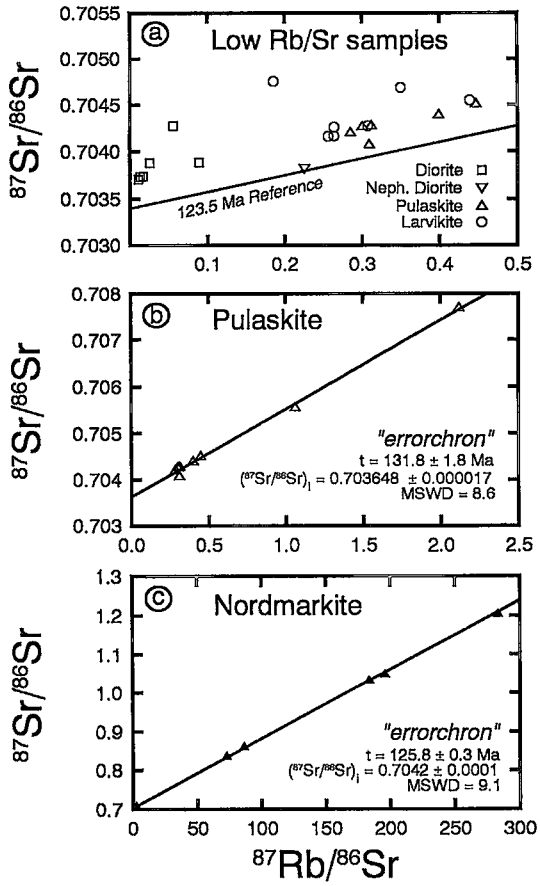

FIG. 7. $^{87}Rb/^{86}Sr$ *versus* $^{87}Sr/^{86}Sr$ isochron diagrams for Shefford samples. (a) All samples with $^{87}Rb/^{86}Sr$ values less than 0.5. Note significant scatter for all rock types. A 123.5-Ma reference isochron (assuming an initial $^{87}Sr/^{86}Sr$ value of 0.7034) is shown. (b) Pulaskite samples (#19 is far off scale). The samples show significant scatter and do not define an isochron. The regression parameters are for an analysis that does not include sample #19. (c) Nordmarkite samples. These samples do not define a valid and reliable isochron because the MSWD is too high.

$^{143}Nd/^{144}Nd$ variations. However, the results are consistent with the age established independently. Similar relationships are observed at other Monteregian complexes (Foland *et al.* 1986).

Significance of the Isotopic Variations

Origin of the isotopic variations

The variations in initial isotopic ratios are interpreted to reflect heterogeneities in the initial magmas. They cannot be the result of alteration that changed the Rb/Sr values long after the formation of the rocks, because samples with low Rb/Sr (*i.e.*, high Sr contents) also exhibit significant variability in the isotopic ratios. The only potential secondary process causing such variations is hydrothermal alteration, whereby more radiogenic Sr is added. Three lines of evidence argue against this. First, variations in $^{143}Nd/^{144}Nd$ are not expected from hydrothermal alteration (*e.g.*, Landoll *et al.* 1994), and $^{143}Nd/^{144}Nd$ inversely correlates with $^{87}Sr/^{86}Sr$, suggesting that the variations in $^{87}Sr/^{86}Sr$ values also are magmatic. Second, the samples are not altered, other than showing typical deuteric effects associated with plutonic rocks. Third, samples with high Sr contents (*e.g.*, diorite and pulaskite) show substantial variations in $^{87}Sr/^{86}Sr$. If the variations are the result of hydrothermal interactions, then very large amounts of Sr would need to be added. The petrography rules out modification of the required magnitude. It is, however, not possible to rule out hydrothermal modification of the $^{87}Sr/^{86}Sr$ values of the nordmarkite, as its Sr content is very low.

The Sr and Nd isotopic ratios define three broad trends (Fig. 6): a mafic trend consisting of the diorite and nepheline diorite; a "saturated" to "undersaturated" trend consisting of the pulaskite and larvikite, and an "oversaturated" one consisting of the nordmarkite. The mafic and saturated to undersaturated groups overlap each other and define a steeper trend of decreasing $^{143}Nd/^{144}Nd$ with moderately increasing $^{87}Sr/^{86}Sr$. The oversaturated trend diverges from the others at lower $^{143}Nd/^{144}Nd$, with a much more gentle slope. As shown below, these trends are consistent with incorporation of crustal material into mantle-derived magmas. The chemical data suggest crystallization from relatively evolved magmas. Thus, the evolution of Shefford is likely to have involved coupled fractional crystallization and assimilation (AFC) processes.

Isotopic composition of the initial magma

The isotopic compositions of the least-contaminated samples are appropriate for a magma produced by melting of a light-*REE*-depleted mantle. Moreover, the $^{143}Nd/^{144}Nd$ values of all Shefford samples (>0.51255) are distinctly higher than the country rock and typical crust (<0.5120), and preclude Shefford from being a direct product of crustal melting (in which case melts would have similar isotopic compositions as their source). This holds for all rock types.

The hypothesis is that all Shefford rocks are ultimately derived from the same parental magma or from closely related ones of virtually the same composition, with the isotopic trends reflecting crustal assimilation. This differs from the interpretation for the Monteregian complexes in general (Eby 1984b, 1985), but is consistent with the similar results for Brome (Chen *et al.* 1994). It is supported by the Sr–Nd isotopic trends that are explained by crustal conta-

mination, and converge toward a common mantle-source value for the parental magma. Additional strong support for this hypothesis is provided by Pb isotopic results for Brome (Wen 1994), where five radiogenic isotopes form consistent and continuous trends and make a common parental composition highly probable.

Considering the entire Shefford data set and the trends, the uncontaminated magma is taken to have $^{87}Sr/^{86}Sr$ and $^{143}Nd/^{144}Nd$ values of 0.70340 and 0.512690, respectively, which is slightly more primitive than the least contaminated sample (#132). The composition originally proposed by Foland *et al.* (1988) is now properly viewed as slightly contaminated. The revised composition for the initial magma is similar to that proposed for the Brome complex by Chen *et al.* (1994).

The distinction of larvikite from nordmarkite

A principal question is whether the larvikite and nordmarkite are different facies of the same unit or different units. The chemical and isotopic data presented in Tables 1 to 4 clearly show substantial compositional distinctions; the nordmarkite is oversaturated and (as discussed below) significantly contaminated, whereas the larvikite is distinctly less saturated and, as judged from isotopic ratios, less strongly contaminated. Therefore, we conclude that the larvikite is not a facies of the nordmarkite.

The larvikite could represent either a separate batch of magma unrelated directly to either a nordmarkitic or pulaskitic magma, or it could be the product of one of these magmas. In the latter case, the larvikite may be a portion of a nordmarkitic or pulaskitic magma that became mixed or contaminated by previously intruded Shefford rocks or magmas, or derived from a pulaskite-like magma that was contaminated by country rock, but not sufficiently to become oversaturated. A confounding factor is that feldspar of apparently cumulate origin occurs in the larvikite. The result is that the chemical composition of the larvikite may differ from the liquid composition, depending on the amount of cumulus feldspar. For example, the compositions of the larvikite samples in Petrogeny's Residua System (Fig. 4) may reflect this factor.

The larvikite shows closer affinities (both chemical and mineralogical) with the pulaskite than with the nordmarkite (*e.g.*, the presence of titanite in some samples). The Sr content of the larvikite is much higher than in the nordmarkite (roughly 800 *versus* 2 ppm) and similar to that in the pulaskite. If sufficient material of dioritic composition were added to a nordmarkitic magma to account for the Sr content of the larvikite, the resulting hybrid magma would not have a larvikite composition. In addition, no microdiorite enclaves were observed in the larvikite. The fact that the larvikite samples have $^{87}Sr/^{86}Sr$ values similar to those in the pulaskite, but lower $^{143}Nd/^{144}Nd$ values (Fig. 6) precludes their derivation from mixtures of pulaskitic and dioritic magmas. Thus, it is probable that the larvikite formed from an originally undersaturated, pulaskitic magma. Its saturation state reflects a small amount of contamination and probably, in part, crystal accumulation.

In many complexes with oversaturated and undersaturated rocks, the oversaturated ones occur on the perimeter, suggesting that the crustal interactions that formed the oversaturated rocks were facilitated by proximity to country rocks. At Shefford, the nordmarkite likewise occurs in an external position (with the larvikite facies generally within, *e.g.*, samples #121 to #128), which supports the proposition that proximity to crustal material was instrumental in forming the quartz syenite.

AFC isotopic models

The Sr and Nd isotopic relationships (variability and inverse correlation) indicate incorporation of crustal material by an assimilation process. Since the chemical relationships indicate that fractional crystallization was important, it is reasonable to regard assimilation and fractional crystallization occurring as a coupled process (AFC). AFC can be modeled readily using observed isotopic ratios. Because many parameters are loosely constrained, no attempt is made to determine unique models. Illustrated models use the apparent isotopic composition of a parental magma, described above, and several contaminant compositions including country-rock samples analyzed in this study, samples of the same formations from near Brome, and a composition for Grenville basement ($^{87}Sr/^{86}Sr$ = 0.715 and 200 ppm Sr, $^{143}Nd/^{144}Nd$ = 0.512 and 30 ppm Nd) estimated from values in the literature (Gilbert 1985). In general, the samples of the Stanbridge Formation have lower $^{143}Nd/^{144}Nd$ and $^{87}Sr/^{86}Sr$ values than those from the Gilman Formation. The model Grenville basement has the same $^{143}Nd/^{144}Nd$ value as the Gilman samples, but a much lower $^{87}Sr/^{86}Sr$ value. Fractional crystallization is accounted for by the bulk distribution coefficients for Sr and Nd. Assimilation is considered at the stages of mafic and more evolved (syenitic) magmatism, with parameters chosen appropriate for each stage. For example, contamination at an evolved stage is modeled using a magma with lower Sr and higher D_{Sr}. Models are shown in Figure 8, and parameters used are summarized in Table 5.

Mafic trend

With relatively high-temperature magmas and country rocks that were previously heated by volcanism, the ratio of assimilation to crystallization (R) at the stage of this mafic magmatism may have been rather high (*e.g.*, 0.5). With crystal fractionation

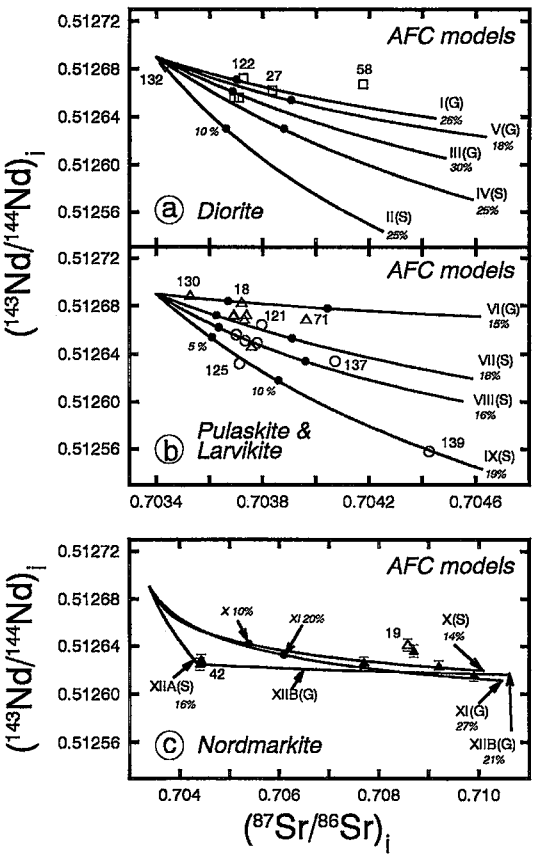

FIG. 8. AFC models based on the initial $^{87}Sr/^{86}Sr$ and $^{143}Nd/^{144}Nd$ values for the three groups of samples (mafic, undersaturated to saturated syenite, oversaturated syenite) discussed in the text. Symbols as in Fig. 2. Parameters for individual models (denoted by Roman numerals) are given in Table 5. The letter following the model number notes whether the crust end-member is Gilman (G) or Stanbridge (S) formations. The numbers under the model number denote the amount of assimilation where the model line terminates. Solid circles denote the amount of assimilation [10% in (a), 5% and 10% in (b), and as noted in (c)]. (a) Diorite samples. Models I and II use identical parameters and display the effect of variations in contaminant composition. (b) Pulaskite and larvikite samples. (c) Nordmarkite samples. Error bars (one sigma) are shown for $^{143}Nd/^{144}Nd$, whereas uncertainties in $^{87}Sr/^{86}Sr$ are variable, but are about ±0.004 for these samples. Note the very different scale for $^{87}Sr/^{86}Sr$ in (c) compared to (a) and (b).

TABLE 5. PARAMETERS USED TO CONSTRUCT AFC MODELS FOR THE MONT SHEFFORD COMPLEX

Model #[a]	Magma[b] Sr	Nd	Crust[c]	D_{Sr}[d]	D_{Nd}[d]	R[e]
I	1700	45	Gilman (44)	1.5	0.2	0.5
II	1700	45	Stanbridge (140)	1.5	0.2	0.5
III	1700	30	Gilman (44)	1.0	0.2	0.5
IV	1200	45	Stanbridge (140)	1.5	0.2	0.5
V	1000	75	Gilman (44)	1.5	0.1	0.3
VI	1000	80	Gilman (44)	2.0	0.5	0.3
VII	1000	80	Stanbridge (140)	1.5	0.5	0.3
VIII	1000	50	Stanbridge (140)	2.0	0.3	0.3
IX	1100	40	Stanbridge (140)	1.5	0.5	0.3
X	750	58	Stanbridge (140)	4.0	0.2	0.2
XI	1000	30	Gilman (44)	3.0	0.15	0.35
XIIA[f]	1000	70	Stanbridge (140)	2.0	0.5	0.35
XIIB[f]	100	80	Gilman (44)	5.0	0.2	0.35
XIII	1700	45	Gilman (44)	2.0	0.15	0.5

[a] Model number refers to Figure 8.

[b] Concentrations of Sr and Nd in the initial magma in ppm.

[c] Crust refers to the country rock sample used as the contaminant. Sample #44 is from the Gilman Formation (east side of Shefford); sample #140 is from the Stanbridge Formation (west side of Shefford). $^{87}Sr/^{86}Sr$, Sr concentration, $^{143}Nd/^{144}Nd$, and Nd concentration of the crust: (0.72900, 150 ppm; 0.511320, 20 ppm) and (0.76600, 70 ppm; 0.51200, 13 ppm) for #140 and #44, respectively.

[d] Bulk distribution coefficients (solid/liquid) for Sr and Nd.

[e] R is the ratio of mass assimilated to mass crystallized.

[f] Models XIIA and XIIB combine in a two-stage model discussed in text. $^{87}Sr/^{86}Sr$ and $^{143}Nd/^{144}Nd$ at beginning of second stage are 0.70440 and 0.51263, respectively.

dominated by plagioclase and clinopyroxene, bulk distribution coefficients for Sr and Nd of 1.0 or 1.5 and 0.2, respectively, are appropriate. Using these parameters, four AFC models are illustrated in Figure 8a in terms of $^{87}Sr/^{86}Sr$ and $^{143}Nd/^{144}Nd$ values.

The two types of country rock (Gilman and Stanbridge) produce significantly different trajectories. For identical parameters, a contaminant with a low $^{87}Sr/^{86}Sr$ value and high Sr content such as the sample of Stanbridge Formation (sample #140) results in a much steeper trajectory than the sample of the Gilman Formation (sample #44), which has a higher $^{143}Nd/^{144}Nd$ value (models I and II, Table 5). For identical parameters used in models I and II, other Gilman samples (from Chen *et al.* 1994, Wen 1994) and the Grenville basement produce trajectories similar to model II. Higher Sr contents of the Stanbridge samples result in trajectories similar to model IV. Thus, the two Shefford country-rock samples provide good end-member compositions for likely contaminants, and subsequent illustrations consider only these two samples for simplicity. This is also consistent with the hypothesis that contamination occurred near the level of intrusion, as suggested by geometrical, lithological, and chemical relationships. Contamination at depth by rocks of appropriate composition cannot be ruled out.

Diorite samples #27 and #122 are readily explained by incorporation of about 10% of crust #44 (model I).

Sample #58 falls to a higher $^{143}Nd/^{144}Nd$ value than predicted by model I. This sample appears to be more felsic than the other diorite samples and can be accounted for by about 17% contamination involving a slightly more evolved magma. Models for these samples involving crust #140 require much less realistic (*e.g.*, very high Nd contents) parameters (*e.g.*, model V, Table 5). Therefore, crust #44 appears to be the likely contaminant for these samples. Diorite samples #26, #134, #59 are bracketed by models III and IV, which suggests that either contaminant could account for their compositions.

In summary, the isotopic compositions of the diorite samples are consistent with evolution involving AFC. Modeling suggests that the parental magma assimilated roughly 10% crustal material. The isotopic data are consistent with crust #44 (Gilman) as being the most likely contaminant for three samples and at least equally likely for the others.

Undersaturated to saturated trend

Several AFC trajectories for the undersaturated to saturated trend are shown in Figure 8b. The isotopic composition of the least-contaminated pulaskite (#130) is very close to that proposed for the parent magma. At least a portion of the parent magma must have undergone considerable fractional crystallization without significant contamination, or the magma chamber was not well mixed and homogenized. Therefore, models for the pulaskite and larvikite use the same initial isotopic composition as for the diorite. The Sr and Nd concentrations, D_{Sr}, and D_{Nd} values used are appropriate for an evolved magma with fractionation of Na-rich plagioclase and minor alkali feldspar (Table 5). The value used for R is 0.3, but the models are insensitive to the value chosen because the amounts of contamination are small.

With an evolved parental magma, both types of country rock must be used to explain the suite of samples. Pulaskite samples #130, #18, #71 are readily explained using crust #44 (model VI), where sample #18 represents about 6% assimilation. Pulaskite samples #72, #120, #29, and #133 and larvikite #121 are best explained by incorporation of 6 to 8% of crust #140 (model VII). Because of its chemical and isotopic affinities with the nordmarkite, pulaskite sample #19 is shown in Figure 8c.

The majority of the larvikite samples are consistent with incorporation of crust #140 (Stanbridge, model VIII). Samples #125 and #139 require a less-evolved magma. The amounts of contamination indicated are about 6 to 8% for both the pulaskite and larvikite (with #139 at 17%), which are similar to, or less than, the diorite. Explaining these samples using crust #44 requires a very low concentration of Nd (less than about 15 ppm) in the initial magma or low D_{Sr} values, both of which are inconsistent with an evolved parental magma.

Both types of country rock are required to explain the full suite of rocks. The geographic locations of the samples broadly correlate with the specific type of country rock required. In general, the pulaskite samples from near or east of the contact zone (Fig. 1) are explained by contamination with the Gilman Formation. Samples #72, #29, #120, and #130 are from near the contact zone and could involve either contaminant. The larvikite samples are generally located west of the inferred contact and are best explained by contamination by the Stanbridge Formation. Because the Gilman Formation probably does not extend to great depth, the above relationships suggest that contamination of the diorite, pulaskite, and larvikite occurred near the present level of exposure. Although stoped blocks or apparent xenoliths are not common in the pulaskite and larvikite, contamination at a high level is also supported by numerous dikes in the larvikite and by complex contact relations with the pulaskite, such as that described for sample #19.

Oversaturated trend

Because calculated initial $^{87}Sr/^{86}Sr$ values of the nordmarkite have large uncertainties (Table 4), the models shown in Figure 8c rely more heavily on $^{143}Nd/^{144}Nd$ values. Successful models must explain: $^{87}Sr/^{86}Sr$ and $^{143}Nd/^{144}Nd$ values that are significantly higher and lower, respectively, than those of the other rock types, a relatively large dispersion in $^{87}Sr/^{86}Sr$ between sample #42 and the other sample of nordmarkite, a relatively flat trend in the correlation of $^{87}Sr/^{86}Sr$ and $^{143}Nd/^{144}Nd$, and very low Sr contents.

The lower $^{143}Nd/^{144}Nd$ and higher $^{87}Sr/^{86}Sr$ of the nordmarkite reflect larger degrees of contamination. The dispersion between #42 (and possibly #87) and the other nordmarkite samples and the relatively constant $^{143}Nd/^{144}Nd$ values require a more complex solution. It is not possible to explain the formation of all nordmarkite samples from the proposed composition of the parent magma with one single-stage model. Either #42 had a separate evolution from the other nordmarkite samples, or the magma experienced a multistage evolution. Alternatively, #42 could have picked up some cognate, more mafic material at a low amount that would not be obvious. Even another alternative is that some $^{87}Sr/^{86}Sr$ values are affected by hydrothermal alteration.

The formation of the high-$^{87}Sr/^{86}Sr$ nordmarkite samples from a syenitic magma similar to that used for the pulaskite is possible using either country rock (models X and XI, Fig. 8c) or Grenville basement. Although the trajectories are similar, these models require very different parameters (Table 5). Model X assumes a slightly more evolved initial magma and a high D_{Sr}, consistent with fractionation of alkali feldspar. In this way, the most contaminated samples

are explained by 12–13% assimilation (and resulting in Sr and Nd concentrations of about 30 and 90 ppm, respectively). In contrast, model XI (crust #44) requires a considerably lower concentration of Nd in the magma and D_{Sr}, and a higher R, which would imply that the initial magma was less evolved. Model XI suggests incorporation of about 24 to 26% crust (Sr and Nd concentrations of about 80–130 and 55 ppm, respectively). Considering the Sr and Nd concentrations of the nordmarkite and the model parameters, model X is preferred. Sample #19 is isotopically similar to nordmarkite #67 and can be explained by similar models of contamination. The slightly higher Sr and lower Nd concentrations of #19 indicate that it consists of highly contaminated pulaskite and did not fractionate to the same extent as the nordmarkite.

Sample #42 can also be explained using either contaminant. Model XIIA is similar to model VIII for the larvikite and uses crust #140. By this model, #42 represents 16% assimilation, with predicted Sr and Nd concentrations of 500 and 80 ppm, respectively. Using crust #44 as a contaminant requires a significantly more mafic parental magma (similar to the parental dioritic magma) and indicates about 23% contamination (Sr and Nd concentrations are 800 and 40 ppm, respectively). Such a model is considered less plausible.

An alternative approach is to consider a multistage evolution. Obviously, such models are more underconstrained of the numerous models that can be constructed; one example is described below. An evolved magma at some depth undergoes AFC involving Stanbridge crust (#140) to produce a magma of a composition similar to that of nordmarkite #42. This magma fractionates, and the Sr concentration decreases to some lower value (*e.g.*, 100 ppm); at this point it is contaminated with Gilman crust (#44) at a shallow level. This is plausible because the Gilman overlies the Stanbridge Formation. Such a scenario is illustrated with models XIIA and XIIB and shown on Figure 8c. In this way, the high-Rb/Sr nordmarkite samples reflect about 21% contamination and have Sr and Nd concentrations of about 35 and 90 ppm, respectively.

The models discussed above adequately account for the isotopic ratios and Nd concentrations of the samples. However, the Sr concentrations of the nordmarkite samples are lower than predicted. Such low concentrations are difficult to reconcile with the isotopic ratios and Nd concentrations by AFC and imply that the Sr concentrations and $^{87}Sr/^{86}Sr$ ratios are decoupled. There are two mechanisms by which this can occur, removal of Sr by hydrothermal fluids, and by fractional crystallization. As major hydrothermal modification of Shefford rocks has already been discounted, fractional crystallization appears to be the only viable explanation.

The evolution of the nordmarkitic magma must have included at least one period of fractional crystallization. The effects of such an evolution ("punctuated AFC") are noted by Landoll *et al.* (1994); assimilation may take place at different intervals of a more continuous history of crystal fractionation. With respect to modeling, punctuated AFC means that the rate of assimilation to fractional crystallization (R) is not constant during the course of magmatic evolution and may approach zero at times, as the magma continuously becomes more evolved. At Shefford, such a scenario is proposed in the two-stage model (XIIA and XIIB, Table 5). Obviously, detailed quantitative analysis beyond that discussed above requires unconstrained speculations regarding the timing and duration of periods of increased or decreased R. However, the low Sr content of the samples requires that significant fractionation must have occurred. Furthermore, the restricted range in the $^{143}Nd/^{144}Nd$ values requires a high D_{Sr}. This trend is consistent with most (if not all) of the fractionation occurring prior to the final stage of contamination.

In sum, AFC involving 12% to 26% crustal input can reasonably account for the observed compositions of the nordmarkite. This amount of contamination, which is principally required by $^{143}Nd/^{144}Nd$ values, is significantly more than for the other rock types. Although the nordmarkite can be explained with both contaminant compositions, crust #140 appears to be more appropriate.

Formation of the Cogenetic Quartz and Nepheline Syenites at Shefford

Several lines of evidence suggest that crustal contamination was instrumental in producing silica-oversaturated rocks at Shefford. For example, the spatial relationships between the amount of contamination and lithology suggest that contamination was facilitated by proximity to country rock. Nordmarkite is invariably found along the perimeter of the complex, whereas undersaturated rocks are generally restricted to interior portions. Where pulaskite is on the perimeter, there is evidence that interactions with country rock took place and the rocks (some of which are oversaturated, *e.g.*, #19) in the area are contaminated. The geographical, temporal, chemical, and isotopic relationships indicate that the quartz- and nepheline-bearing syenites are related and possibly formed from a common evolved magma. This is possible with contamination of an undersaturated felsic magma that can evolve across the Ab–Or join to oversaturation (Foland *et al.* 1993).

A relationship between contamination and degree of saturation is indicated by a correlation of isotope ratios with bulk composition. For example, there is a correlation between initial $^{87}Sr/^{86}Sr$ and $^{143}Nd/^{144}Nd$ values with SiO_2 (Fig. 9). It is clear that the high-SiO_2

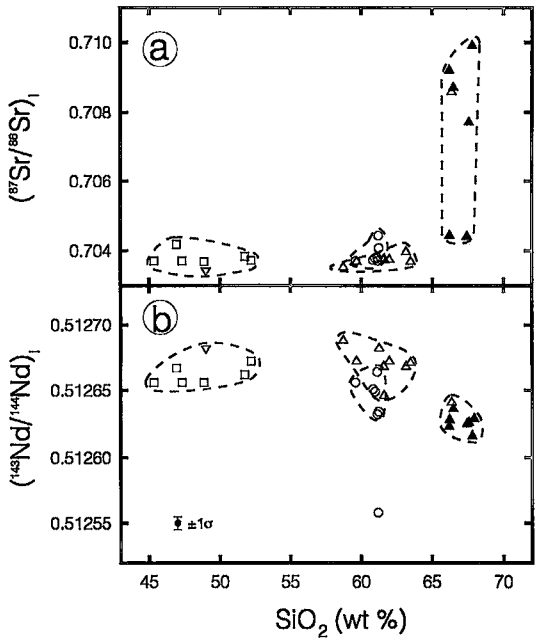

FIG. 9. Initial $^{87}Sr/^{86}Sr$ (a) and $^{143}Nd/^{144}Nd$ values (b) *versus* SiO_2 for Shefford samples. Fields are drawn around samples of different lithologies. Symbols as in Fig. 2. Note the correlation of initial ratio with lithology. The nordmarkite samples have the highest $^{87}Sr/^{86}Sr$ and lowest $^{143}Nd/^{144}Nd$ values. The larvikite samples also have slightly elevated $^{87}Sr/^{86}Sr$ and depressed $^{143}Nd/^{144}Nd$ values relative to the "uncontaminated" pulaskite and diorite samples.

rocks (nordmarkite) are the most contaminated. In addition, the larvikite is slightly contaminated. Two larvikite samples have an isotopic ratio similar to the nordmarkite, and a third highly contaminated sample has a considerably lower $^{143}Nd/^{144}Nd$ value. Except for sample #19, the pulaskite has fairly uniform initial $^{143}Nd/^{144}Nd$ and $^{87}Sr/^{86}Sr$ values. Sample #19 is highly contaminated and also is oversaturated, although it is similar to the pulaskite in many other respects. Undersaturated rocks that are contaminated are not inconsistent with the hypothesis proposed above, but are probably common (*e.g.*, Landoll *et al.* 1994). If contamination ceased before a magma became oversaturated, then undersaturated magmas would bear the effects of contamination. Similarly, if contamination occurred at a late stage of evolution, after a magma had become considerably undersaturated, it could not cause the magma to become oversaturated.

AFC residua system models

Crystallization of a felsic magma is largely controlled by the phase relations in Petrogeny's Residua System, in which oversaturated and undersaturated compositions are separated by the Ab–Or join (Fig. 10). In this phase-equilibrium system, melts that are oversaturated in silica (plotting above the join) fractionate toward the granite minimum, whereas those undersaturated (below the join) evolve by fractionation toward the phonolite minimum. By fractionation alone (except for the rare case of leucite effects: Fudali 1963), a liquid cannot produce both oversaturated and undersaturated compositions, thus posing an apparent dilemma in explaining cogenetic quartz-bearing and nepheline-bearing syenites. Recently, chemical mass-balance models for AFC in the residua system have been constructed to explain such associations under the constraints of equilibrium phase-relations (Foland *et al.* 1993, Landoll *et al.* 1994). In terms of the residua system, whereas fractional crystallization causes an undersaturated felsic magma to follow a path toward the phonolite minimum, assimilation of granitic material will cause it to move toward the granite minimum. AFC results in compositions intermediate between these two and produces curved paths of liquid descent that can cross the feldspar join. This is because the join is not isothermal, but rather has a minimum near the composition Or_{30}, and thus the join does not act as a divide under AFC. The model compositional paths are ones of decreasing temperature. The general models presented below demonstrate the efficacy of producing the oversaturated rocks at Shefford from a felsic undersaturated magma and also estimate the amount of contamination required.

The pertinent model-parameters need explanation. The composition assumed for the uncontaminated "parental" syenitic magma is $Qtz_{44}Ne_{35}Ks_{21}$. This composition is similar to that of the most potassic undersaturated pulaskite sample (#71), but is slightly more undersaturated. The contaminant is taken to be the composition of a minimum-melt granite, which is appropriate for assimilation of either a partial melt or solid blocks of granitic crust. Whereas changes in R during evolution can readily be modeled and may be more realistic, such models require detailed information on the timing of the changes. Without such information, constant values of R (0.2 and 0.35) are used, and separate models are constructed using different values based on the isotopic models given above. The fractionating feldspars are assumed to be in equilibrium with the liquid from which they crystallize; their compositions are determined graphically using crystal–liquid tie lines inferred from the fractionation paths of Tuttle & Bowen (1958) and Hamilton & MacKenzie (1965), as explained in Landoll *et al.* (1994). In short, as undersaturated magmas approach the Ab–Or join during AFC, the feldspars become more potassic; once across the join, they become more sodic as the melt moves toward the granite minimum.

The construction of a model that explains the

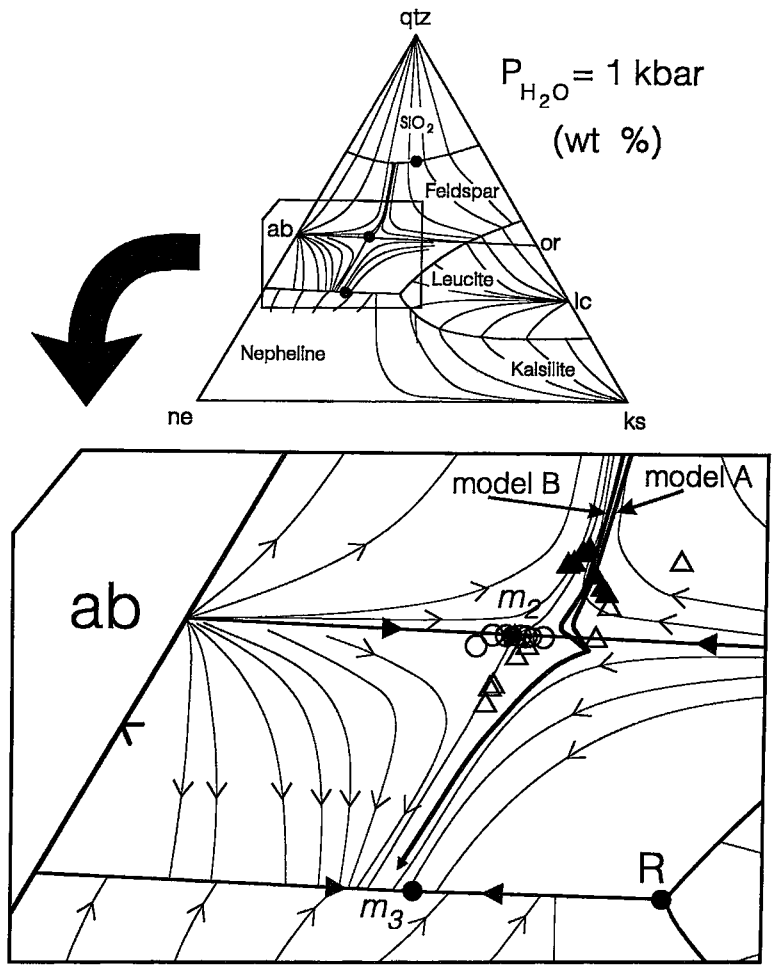

FIG. 10. Compositions of felsic samples and calculated paths of liquid evolution in terms of Petrogeny's Residua System. The reference triangle at the top shows phase-boundary curves, minima (solid dots), and paths of fractional crystallization for $P(H_2O)$ = 1 kbar [paths of fractional crystallization from Tuttle & Bowen (1958), Fudali (1963), and Hamilton & MacKenzie (1965)]. The enlargement also shows calculated paths of liquid evolution (dark lines) for AFC and fractional crystallization of an initial, undersaturated magma. AFC model A assumes a constant ratio of assimilation to fractionation of 0.2; model B assumes a constant ratio of 0.35. Samples are projected into this system using CIPW norms, as explained in the text. Note the positions of samples #19, #71, and #72 as discussed in the text and Fig. 4. Symbols as in Fig. 2.

compositions of all samples is not realistic, because some samples apparently do not approximate liquid compositions. For example, the larvikite samples plot along the feldspar join on both sides of the minimum (m_2, Fig. 4), which suggests that either there were two "parental larvikite" magmas or that the larvikite contains Na-rich cumulate (or xenocrystic) material. The larvikite contains partially resorbed crystals of plagioclase and, therefore, samples do not represent liquid compositions. Likewise, pulaskite #19 is highly anomalous and may have accumulated alkali feldspar. Therefore, chemical models do not attempt to produce their compositions. Accumulation of crystals in equilibrium with a melt will alter the chemical but not the isotopic compositions, and decouples the chemical and isotopic systems.

Two calculated AFC-dominated liquid paths that reasonably explain the formation of the nordmarkite in a general manner are shown in Figure 10. The AFC trajectories cross the feldspar join near its thermal minimum and basically follow the thermal trough. Because of this, the models are rather insensitive to the value of *R*. This is shown by the similar trajectories of the two models in Figure 10. In fact, once the magma crosses into the granite pseudoternary system, even an *R* of zero (pure fractional crystallization) produces a trajectory that is only slightly different (Fig. 10; Tuttle & Bowen 1958). For both models shown in Figure 10, about 4% contamination is required to reach the feldspar minimum; however, model A does so with about 82% of the melt remaining, whereas in model B, about 91% liquid is present when the join is crossed. The most silica-rich samples are explained by about 15% contamination for model A and about 20% for model B.

Of course, for pure fractional crystallization, an undersaturated magma will evolve along a curved path toward the thermal valley and away from the feldspar join (Fig. 10). However, most of the pulaskite samples are richer in SiO_2 than this trajectory. This is consistent with a small amount of contamination, as indicated by the isotopic data (Fig. 8). The contamination could have occurred early, which suggests either a low value of *R* or a small amount of contamination (*i.e.*, less than 4%). Conversely, the contamination could have occurred late, after the magma had become too strongly undersaturated to cross the divide regardless of the amount of contamination (Landoll *et al.* 1994).

In summary, the chemical models are consistent with production of the nordmarkite by AFC from the same undersaturated syenitic magma that formed the pulaskite. Because the magma evolved near the thermal trough, differences between the effects of fractional crystallization and AFC are obscured once the magma crossed the feldspar join. The isotopic models broadly agree with the chemical models and indicate about 15–20% contamination for the most strongly contaminated nordmarkite samples. The pulaskite formed principally by fractional crystallization, with only minor amounts of contamination. Although not conclusive, the Stanbridge Formation (as represented by sample #140) seems to be a more likely candidate for the contaminant, on the basis of the isotopic data.

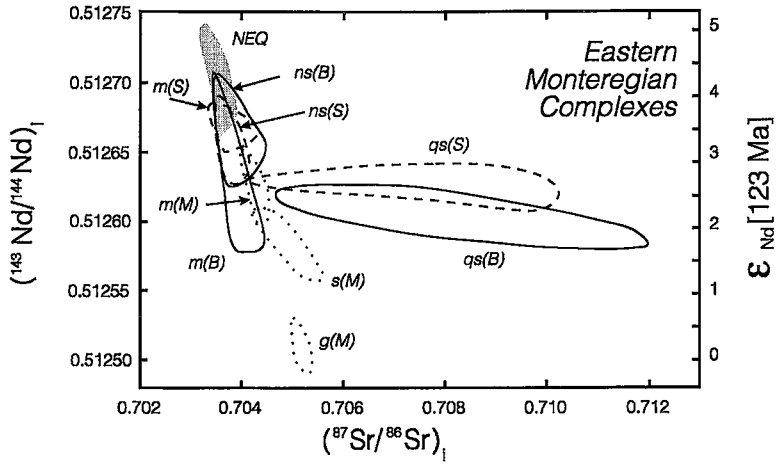

FIG. 11. Initial $^{87}Sr/^{86}Sr$ *versus* $^{143}Nd/^{144}Nd$ values for the eastern Monteregian complexes, Mont Shefford, Mont Brome, and Mont Megantic, showing the similarities in the isotopic relations. Fields for individual lithologies are shown with different types of lines and are labeled as follows. Mont Shefford: long dashed line; m(S): mafic rocks, ns(S): nepheline syenite and larvikite (note sample #139, $^{143}Nd/^{144}Nd = 0.512558$, is not included), qs(S): oversaturated syenites. Mont Brome: solid line; m(B): mafic rocks, ns(B): nepheline syenites, qs(B): oversaturated syenites. Mont Megantic: short dashed line; m(M): mafic rocks, s(M): syenite, g(M): granite. The shaded field gives the compositions of least-contaminated rocks of the other Monteregian Hills province and Cretaceous White Mountain complexes [from Foland *et al.* (1988), with modifications from unpublished data]. The inferred compositions of parental magmas from each complex are similar and suggest similar sources in the mantle. The country rock and basement have $^{143}Nd/^{144}Nd$ values that are much lower than these Monteregian intrusive complexes (Fig. 6 and text). The negatively correlated isotopic ratios indicate contamination, with significantly larger crustal components in the oversaturated rocks. Data for Mont Brome from Chen *et al.* (1994), and Mont Megantic, from Foland & Chen (unpubl. data).

Extension to Other Monteregian Complexes

Oversaturated rocks also occur in other Monteregian complexes, particularly the eastern complexes of Mont Brome and Mont Megantic (Bédard *et al.* 1987). The $^{87}Sr/^{86}Sr$ and $^{143}Nd/^{144}Nd$ values are compared for Mont Shefford, Mont Brome, and Mont Megantic in Figure 11. For all three complexes, the mafic and undersaturated rocks have similar ratios and point to a mantle source(s), with time-integrated depletion. Compositions trend away from apparent mantle values (near $^{143}Nd/^{144}Nd$ about 0.5127 and $^{87}Sr/^{86}Sr$ about 0.7035) and toward crustal values within the field for magmas parental to related complexes.

For all three complexes, the quartz-bearing rock types extend to substantially lower $^{143}Nd/^{144}Nd$ and higher $^{87}Sr/^{86}Sr$ values than do undersaturated lithologies. These trends are interpreted to reflect incorporation of crustal material *via* AFC-type processes. The country rocks and basement have substantially lower $^{143}Nd/^{144}Nd$ values and thus the quartz-bearing felsic rocks cannot be the direct products of crustal anatexis.

Thus, the isotopic compositions of all three Monteregian intrusive complexes that contain oversaturated felsic rocks are consistent with the type of contamination processes found for Shefford. In all cases, larger crustal components are indicated for the oversaturated rocks. The Brome and Shefford complexes obviously present very similar relationships. Although Nd isotopic data are more limited for Megantic, initial ratios for the complexes appear to converge toward a common value, indicating derivation of their parental magmas from common a (or at least isotopically similar) mildly light-*REE*-depleted mantle source. In addition, the geometries of the complexes, where oversaturated rocks are on the perimeter and undersaturated ones in the interior, holds for locations that contain undersaturated rocks. In each case, the relations are consistent with formation of the oversaturated rocks by AFC from the same undersaturated felsic magma that produced the nepheline syenites. This demonstrates the widespread importance of combined assimilation and fractionation processes (*e.g.*, Foland *et al.* 1993, Landoll *et al.* 1992, 1994, Landoll 1994) for producing oversaturated rock-types.

Conclusions

The relationships at Mont Shefford are consistent with all rock types being cogenetic. The compositions in terms of major and trace elements are consistent with formation of the syenitic rocks from a mafic melt *via* fractional crystallization. The two facies of the nordmarkite unit as mapped (nordmarkite and larvikite) are mineralogically, chemically, and isotopically distinct. The larvikite has closer affinities with the pulaskite, and probably formed from a similar undersaturated magma. The Sr and Nd isotopic relationships indicate a mantle source with a time-integrated, mildly light-*REE*-depleted signature. The $^{143}Nd/^{144}Nd$ values of the nordmarkite show that it is not the direct product of crustal anatexis, as has been previously suggested. Close similarities in the chemical and isotopic relationships between Shefford and the nearby Mont Brome complex suggest that they formed from similar materials by similar processes.

Significant variations occur in initial $^{87}Sr/^{86}Sr$ and $^{143}Nd/^{144}Nd$ values, which preclude dating the complex by the Rb–Sr whole-rock method, and indicate contamination of the magmas with crustal material. AFC models indicate that contamination occurred at different stages (mafic and evolved), and that some magma evolved to a syenitic stage without significant contamination. The amounts of contamination correlate with rock type and show that the nordmarkite was the most affected. The contamination apparently occurred at a high crustal level, perhaps near the level of intrusion. Although equivocal, the Stanbridge Formation appears to be the dominant contaminant.

Several relationships at Shefford (*e.g.*, distribution of lithologies, correlation of isotopes with degree of saturation) indicate that the saturated and oversaturated rocks formed by contamination processes. Chemical models demonstrate the ability of AFC and fractional crystallization with equilibrium compositions to produce both the oversaturated and undersaturated rocks from the same undersaturated syenitic initial magma. Similar processes seem to be responsible for the formation of these associations at other Monteregian Hills localities and in alkaline complexes more generally.

Acknowledgements

The authors thank collaborator C.M.B. Henderson for results of chemical analyses and discussions, and colleagues F.A. Hubacher and J.S. Linder for vital support in the laboratory. Reviews, comments, and suggestions by J. Bédard, M. Dorais, an anonymous reviewer, R.F. Martin and, especially, L. Corriveau, were extremely valuable. Financial support was provided, in part, by NSF grants EAR–8708008 and EAR–9018042, NATO grant RG–86/0017, and a Graduate Student Research Award from the Graduate School of Ohio State University to JDL. The mass spectrometer used for this study was acquired with NSF grant EAR–8419126.

References

Bédard, J.H.J., Ludden, J.N. & Francis, D.M. (1987): The Megantic intrusive complex, Quebec: a study of the derivation of silica-oversaturated anorogenic magmas of alkaline affinity. *J. Petrol.* **28**, 355-388.

BROOKS, C., HART, S.R. & WENDT, I. (1972): Realistic use of two-error regression treatment as applied to rubidium–strontium data. *Rev. Geophys. Space Phys.* **10**, 551-577.

CHEN, JAING-FENG, HENDERSON, C.M.B. & FOLAND, K.A. (1994): Open-system subvolcanic magmatic evolution: constraints on the petrogenesis of the Mount Brome alkaline complex, Canada. *J. Petrol.* **35**, 1127-1153.

DOOLAN, B.L., GALE, M.H., GALE, P.N. & HOAR, R.S. (1982): Geology of the Quebec re-entrant: possible constraints from early rifts and the Vermont–Quebec serpentine belt. *In* Major Structural Zones and Faults of the Northern Appalachian (P. St-Julien & J. Béland, eds.). *Geol. Assoc. Can., Spec. Pap.* **24**, 87-115.

EBY, G.N. (1984a): Geochronology of the Monteregian Hills alkaline igneous province. *Geology* **12**, 468-470.

_____ (1984b): Monteregian Hills. I. Petrography, major and trace element geochemistry, and strontium isotopic geochemistry of the western intrusions: Mounts Royal, St. Bruno, and Johnson. *J. Petrol.* **25**, 421-452.

_____ (1985): Monteregian Hills. II. Petrography, major and trace element geochemistry, and strontium isotopic geochemistry of the eastern intrusions: Mount Shefford, Brome, and Megantic. *J. Petrol.* **26**, 418-448.

_____ (1987): The Monteregian Hills and White Mountain alkaline igneous provinces, eastern North America. *In* Alkaline Igneous Rocks (J.G. Fitton & B.G.J. Upton, eds.). *Geol. Soc., Spec. Publ.* **30**, 433-447.

FOLAND, K.A. & ALLEN, J.C. (1991): Magma sources for Mesozoic anorogenic granites of the White Mountain magma series, New England, USA. *Contrib. Mineral. Petrol.* **109**, 195-211.

_____, CHEN, JAING-FENG, GILBERT, L.A. & HOFMANN, A.W. (1988): Nd and Sr isotopic signatures of Mesozoic plutons in northeastern North America. *Geology* **16**, 684-687.

_____, _____, LINDER, J.S., HENDERSON, C.M.B. & WHILLANS, I.M. (1989): High-resolution $^{40}Ar/^{39}Ar$ chronology of multiple intrusion igneous complexes: application to the Cretaceous Mount Brome complex, Quebec, Canada. *Contrib. Mineral. Petrol.* **102**, 127-137.

_____, GILBERT, L.A., SEBRING, C.A. & CHEN, JAING-FENG (1986): $^{40}Ar/^{39}Ar$ ages for plutons of the Monteregian Hills, Quebec: evidence for a single episode of Cretaceous magmatism. *Geol. Soc. Am., Bull.* **97**, 966-974.

_____, LANDOLL, J.D., HENDERSON, C.M.B. & CHEN, JAING-FENG (1993): Formation of cogenetic quartz and nepheline syenites. *Geochim. Cosmochim. Acta* **57**, 697-704.

FRISCH, T. (1970): Chemical variations among the amphiboles of Shefford Mountain, a Monteregian intrusion in southern Quebec. *Can. Mineral.* **10**, 553-570.

FUDALI, R.F. (1963): Experimental studies bearing on the origin of pseudoleucite and associated problems of alkalic rock systems. *Geol. Soc. Am., Bull.* **74**, 1101-1126.

GILBERT, L.A. (1985): *Petrogenesis of the Mont Saint-Hilaire Alkaline Igneous Complex, Quebec.* M.S. thesis, Ohio State Univ., Columbus, Ohio.

GREENWOOD, R.C. & EDGAR, A.D. (1984): Petrogenesis of the gabbros from Mt. St. Hilaire, Quebec, Canada. *Geol. J.* **19**, 353-376.

HAMILTON, D.L. & MACKENZIE, W.S. (1965): Phase-equilibrium studies in the system $NaAlSiO_4$ (nepheline) – $KAlSiO_4$ (kalsilite) – SiO_2 – H_2O. *Mineral. Mag.* **34**, 214-231.

HARPER, C.L. (1988): *On the Nature of Time in Cosmological Perspective.* Ph.D. dissertation, Oxford Univ., Oxford, U.K.

HENDERSON, C.M.B. (1984): Feldspathoid stabilities and phase inversions – a review. *In* Feldspar and Feldspathoids, Structures, Properties and Occurrences (W.L. Brown, ed.). Reidel, Dordrecht, The Netherlands.

LANDOLL, J.D. (1994): *The Role of Crustal Interactions in the Formation of Cogenetic Silica Oversaturated and Undersaturated Syenites: Evidence from the Alkaline Complexes of Abu Khruq (Egypt), Mt. Shefford (Quebec), and Marangudzi (Zimbabwe).* Ph.D. dissertation, Ohio State Univ., Columbus, Ohio.

_____, FOLAND, K.A. & HENDERSON, C.M.B. (1992): Formation of cogenetic silica over- and undersaturated syenites: evidence from several localities. *Geol. Soc. Am., Abstr. Programs* **24**, A217.

_____, _____, _____ (1994): Nd isotopes demonstrate the role of contamination in the formation of coexisting quartz and nepheline syenites at the Abu Khruq Complex, Egypt. *Contrib. Mineral. Petrol.* **117**, 305-329.

MIYASHIRO, A. (1978): Nature of alkalic volcanic rock series. *Contrib. Mineral. Petrol.* **66**, 91-104.

PHILPOTTS, A.R. (1970): Mechanism of emplacement of the Monteregian Hills. *Can. Mineral.* **10**, 395-410.

RICKARD, M.J. (1991): Stratigraphy and structural geology of the Cowansville – Sutton – Mansonville area in the Appalachians of southern Quebec. *Geol. Surv. Can., Pap.* **88-27**.

SÉGUIN, M.K. (1982): Emplacement of the Monteregian Hills of Quebec: geophysical evidence. *Tectonophys.* **86**, 305-317.

SLIVITZKY, A. & ST-JULIEN, P. (1987): Compilation géologique de la région de l'Estrie – Beauce. *Ministère des Richesses Naturelles du Québec, Rapp.* **MM 85-04**.

TUTTLE, O.F. & BOWEN, N.L. (1958): Origin of granite in the light of experimental studies in the system $NaAlSi_3O_8$ – $KAlSi_3O_8$ – SiO_2 – H_2O. *Geol. Soc. Am., Mem.* **74**.

VALIQUETTE, G. & POULIOT, G. (1977): Geology of Mounts Brome and Shefford. *Ministère des Richesses Naturelles du Québec, Rapp.* **ES-28**.

WEN, D. (1994): *Lead Isotope Constraints on the Petrogenesis of the Mount Brome Alkaline Complex.* M.S. thesis, Ohio State Univ., Columbus, Ohio.

Received September 15, 1994, revised manuscript accepted October 20, 1995.